Fatty acid oxidation participates in resistance to nutrient-depleted environments in the insect stages of Trypanosoma cruzi

Rodolpho Ornitz Oliveira Souza, Flávia Silva Damasceno, Sabrina Marsiccobetre, Marc Biran, Gilson Murata, Rui Curi, Frédéric Bringaud, Ariel Mariano Silber

PLOS PATHOGENS

RESEARCH ARTICLE

Fatty acid oxidation participates in resistance to nutrient-depleted environments in the insect stages of *Trypanosoma cruzi*

Rodolpho Ornitz Oliveira Souza[1], Flávia Silva Damasceno[1], Sabrina Marsiccobetre[1], Marc Biran[2], Gilson Murata[3], Rui Curi[3,4], Frédéric Bringaud[5], Ariel Mariano Silber[1]*

1 University of São Paulo, Laboratory of Biochemistry of Tryps–LaBTryps, Department of Parasitology, Institute of Biomedical Sciences–São Paulo, São Paulo, Brazil, **2** Centre de Résonance Magnétique des Systèmes Biologiques (RMSB), Université de Bordeaux, Bordeaux, France, **3** University of São Paulo, Department of Physiology, Institute of Biomedical Sciences–São Paulo, São Paulo, Brazil, **4** Cruzeiro do Sul University, Interdisciplinary Post-Graduate Program in Health Sciences—São Paulo, São Paulo, Brazil, **5** Laboratoire de Microbiologie Fondamentale et Pathogénicité (MFP), Université de Bordeaux, Bordeaux, France

* asilber@usp.br

OPEN ACCESS

Citation: Souza ROO, Damasceno FS, Marsiccobetre S, Biran M, Murata G, Curi R, et al. (2021) Fatty acid oxidation participates in resistance to nutrient-depleted environments in the insect stages of *Trypanosoma cruzi*. PLoS Pathog 17(4): e1009495. https://doi.org/10.1371/journal.ppat.1009495

Editor: Michael L. Ginger, University of Huddersfield, UNITED KINGDOM

Received: January 15, 2021

Accepted: March 23, 2021

Published: April 5, 2021

Data Availability Statement: All relevant data are within the manuscript and its Supporting Information files.

Funding: This work was supported by Fundação de Amparo à Pesquisa do Estado de São Paulo (www.fapesp.br) grants 2016/06034-2 and 2018/14432-3 (awarded to AMS); Conselho Nacional de Desenvolvimento Científico e Tecnológico (www.cnpq.br/) grants 308351/2013-4 and 404769/2018-7 (awarded to AMS), Research Council

Abstract

Trypanosoma cruzi, the parasite causing Chagas disease, is a digenetic flagellated protist that infects mammals (including humans) and reduviid insect vectors. Therefore, *T. cruzi* must colonize different niches in order to complete its life cycle in both hosts. This fact determines the need of adaptations to face challenging environmental cues. The primary environmental challenge, particularly in the insect stages, is poor nutrient availability. In this regard, it is well known that *T. cruzi* has a flexible metabolism able to rapidly switch from carbohydrates (mainly glucose) to amino acids (mostly proline) consumption. Also established has been the capability of *T. cruzi* to use glucose and amino acids to support the differentiation process occurring in the insect, from replicative non-infective epimastigotes to non-replicative infective metacyclic trypomastigotes. However, little is known about the possibilities of using externally available and internally stored fatty acids as resources to survive in nutrient-poor environments, and to sustain metacyclogenesis. In this study, we revisit the metabolic fate of fatty acid breakdown in *T. cruzi*. Herein, we show that during parasite proliferation, the glucose concentration in the medium can regulate the fatty acid metabolism. At the stationary phase, the parasites fully oxidize fatty acids. [U-^{14}C]-palmitate can be taken up from the medium, leading to CO_2 production. Additionally, we show that electrons are fed directly to oxidative phosphorylation, and acetyl-CoA is supplied to the tricarboxylic acid (TCA) cycle, which can be used to feed anabolic pathways such as the *de novo* biosynthesis of fatty acids. Finally, we show as well that the inhibition of fatty acids mobilization into the mitochondrion diminishes the survival to severe starvation, and impairs metacyclogenesis.

United Kingdom Global Challenges Research Fund under grant agreement "A Global Network for Neglected Tropical Diseases" (https://www.ukri.org/research/global-challenges-research-fund/) (grant MR/P027989/1) (awarded to AMS). In addition, FB was supported by the Université de Bordeaux (https://www.u-bordeaux.fr/), the Centre National de la Recherche Scientifique (CNRS, http://www.cnrs.fr/), the Agence Nationale de la Recherche (ANR, http://www.agence-nationale-recherche.fr) through GLYCONOV and ADIPOTRYP grants of the "Générique » call and the Laboratoire d'Excellence (LabEx) ParaFrap ANR-11-LABX-0024. The funders had no role in study design, data collection and analysis, decision to publish, or preparation of the manuscript.

Competing interests: The authors have declared that no competing interests exist.

Author summary

Trypanosoma cruzi is a protist parasite with a life cycle involving two types of hosts, a vertebrate one (which includes humans, causing Chagas disease) and an invertebrate one (kissing bugs, which vectorize the infection among mammals). In both hosts, the parasite faces environmental challenges such as sudden changes in the metabolic composition of the medium in which they develop, severe starvation, osmotic stress and redox imbalance, among others. Because kissing bugs feed infrequently in nature, an intriguing aspect of *T. cruzi* biology (it exclusively inhabits the digestive tube of these insects) is how they subsist during long periods of starvation. In this work, we show that this parasite performs a metabolic switch from glucose consumption to lipid oxidation, and it is able to consume lipids and the lipid-derived fatty acids from both internal origins as well as externally supplied compounds. When fatty acid oxidation is chemically inhibited by etomoxir, a very well-known drug that inhibits the translocation of fatty acids into the mitochondria, the proliferative insect stage of the parasites has dramatically diminished survival under severe metabolic stress and its differentiation into its infective forms is impaired. Our findings place fatty acids in the centre of the scene regarding their extraordinary resistance to nutrient-depleted environments.

Introduction

T. cruzi, a flagellated parasite, is the causative agent of Chagas disease, a neglected health problem endemic to the Americas [1]. The parasite life cycle is complex, alternating between replicative and non-replicative forms in two types of hosts, mammalians and triatomine insects [2]. In mammalian hosts, two primary forms are recognized: replicative intracellular amastigotes and nondividing trypomastigotes, which are released from infected host cells into the extracellular medium. After being released from infected cells, trypomastigotes can spread the infection by infecting new cells, or they can be ingested by a triatomine bug during its blood meal. Once inside the invertebrate host, the ingested trypomastigotes differentiate into epimastigotes, which initiate their proliferation and colonization of the insect digestive tract [3]. Once the epimastigotes reach the final portion of the digestive tube, they initiate differentiation into non-proliferative, infective metacyclic trypomastigotes. These forms will be expelled during a new blood meal and will be able to infect a new vertebrate host [2,4–6].

The diversity of environments through which *T. cruzi* passes during its life cycle (i.e., the digestive tube of the insect vector, the bloodstream and the mammalian cells cytoplasm) subjects it to different levels of nutrient availability [3,7]. Therefore, this organism evolved a robust, flexible and efficient metabolism [4,8]. As an example, it was recognized early on that epimastigotes are able to rapidly switch their metabolism, allowing the consumption of carbohydrates and different amino acids [9,10]. Several studies identified aspartate, asparagine, glutamate [11], proline [12–14], histidine [15], alanine [11,16] and glutamine [11,17] as oxidisable energy sources.

T. cruzi glycolysis is by far the most studied metabolic pathway in trypanosomatids. It happens in a specific peroxisome-related organelles named glycosomes and the cytosol [18,19]. The absence of the classical controls by ATP and O_2 (Pasteur effect) is compensated by such compartmentalization [18]. It has been suggested that glycosomes do not exchange ATP and glycolytic cofactors such as NAD (H) with the cytosol [20]. Therefore, the intra-glycosomal ATP/ADP ratio prevents the deleterious effects of the uncontrolled activation of ATP-dependent glycolytic enzymes (hexokinase and phosphofructokinase) by the surplus ATP which is

produced in the cytoplasm, the denominated "turbo design" [21]. In addition, many pathways contribute to maintain the intra-glycosomal redox balance. A remarkable one consists in the conversion of phosphoenolpyruvate into succinate, a NADH reoxidizing pathway which includes a cytosolic shunt, involving a cytosolic fumarase, and finally a glycosomal fumarate reductase [22]. The last two enzymes are responsible for part of the reoxidation of NADH [22]. This pathway produces significant amounts of succinate, a main end product of *T*. *cruzi* glycolysis. Pyruvate can be also a substrate of transaminases as a $-NH_2$ acceptor, resulting in formation of alanine that is exported from the cell, or can be imported into the mitochondrion where the pyruvate dehydrogenase complex can convert it into Acetyl-CoA and subsequently into acetate, which can be excreted. Acetyl-CoA can be also incorporated into the TCA cycle, to produce reducing equivalents for the mitochondrial respiratory chain and carbon skeletons for producing other metabolites. Importantly, there is a mitochondrial isoform of fumarate reductase, which, as happens with its glycosomal counterpart, is able to convert mitochondrial fumarate into succinate. Much less is known about how *T*. *cruzi* uses fatty acids and how these compounds contribute to the parasite´s metabolism and survival. The $NADP^+$-dependent β-oxidation of palmitoyl-CoA has been shown in mitochondrial and glycosomal fractions of *T*. *cruzi* epimastigotes [23], and a recent proteomic analysis of glycosomes showed the presence of all the required enzymes for this process [24]. In this study, we explore fatty acid metabolism in *T*. *cruzi*. We also address fatty acid regulation by external glucose levels and the involvement of their oxidation in the replication and differentiation of *T*. *cruzi* insect stages.

Methods

Parasites

Epimastigotes of *T*. *cruzi* strain CL clone 14 were maintained in the exponential growth phase by sub-culturing them for 48 h in Liver Infusion Tryptose (LIT) medium at 28˚C [25]. Metacyclic trypomastigotes were obtained through the differentiation of epimastigotes at the stationary growth phase by incubation for 2 h in TAU (Triatomine Artificial Urine) medium (190 mM NaCl, 8 mM phosphate buffer pH 6.0, 17 mM KCl, 2 mM $CaCl_2$, 2 mM $MgCl_2$) followed by an incubation for 6 days in TAU-3AAG (TAU supplemented with 10 mM proline, 50 mM glutamate, 2 mM aspartate and 10 mM glucose) as previously reported [17], or TAU-3AAG supplemented with 5, 10, 25 or 50 mM etomoxir (ETO).

Fatty acid oxidation assays

Preparation of palmitate-BSA conjugates. Sodium palmitate at 70 mM was solubilized in water by heating it up to 70˚C. BSA free fatty acids (FFA BSA) (Sigma Aldrich) was dissolved in PBS and warmed up to 37˚C with continuous stirring. Solubilized palmitate was added to BSA at 37˚C with continuous stirring (for a final concentration of 5 mM in 7% BSA). The conjugated palmitate-BSA was aliquoted and stored at −80˚C [26].

CO_2 production from oxidisable carbon sources. To test the production of CO_2 from palmitate, glucose or histidine, exponentially growing epimastigotes ($5x10^7$ mL^{-1}) were washed twice in PBS and incubated for different times (0, 30, 60 and 120 min) in the presence of 0.1 mM of palmitate spiked with 0.2 μCi of ^{14}C-U-substrates. To trap the produced CO_2, Whatman paper was embedded in 2 M KOH solution and was placed in the top of the tube. The $^{14}CO_2$ trapped by this reaction was quantified by scintillation [15,16].

^{1}H-NMR analysis of the exometabolome. Epimastigotes ($1x10^8$ mL^{-1}) were collected by centrifugation at 1,400 x *g* for 10 min, washed twice with PBS and incubated in 1 mL (single point analysis) of PBS supplemented with 2 g/L $NaHCO_3$ (pH 7.4). The cells were maintained for 6 h at 27˚C in incubation buffer containing [U-^{13}C]-glucose, non-enriched palmitate or no

carbon sources. The integrity of the cells during the incubation was checked by microscopic observation. The supernatant (1 mL) was collected and 50 μl of maleate solution in D_2O (10 mM) was added as an internal reference. ^{1}H-NMR spectra were collected at 500.19 MHz on a Bruker Avance III 500 HD spectrometer equipped with a 5 mm Prodigy cryoprobe. The measurements were recorded at 25˚C. The acquisition conditions were as follows: 90˚ flip angle, 5,000 Hz spectral width, 32 K memory size, and 9.3 sec total recycling time. The measurements were performed with 64 scans for a total time of close to 10 min and 30 sec. The resonances of the obtained spectra were integrated and the metabolite concentrations were calculated using the ERETIC2 NMR quantification Bruker program.

Oxygen consumption. To evaluate the importance of internal fatty acid sources in O_2 consumption, exponentially growing parasites were treated or not treated with 500 μM ETO (the inhibitor of carnitine palmitoyltransferase 1), washed twice in PBS and resuspended in Mitochondrial Cellular Respiration (MCR) buffer. The rates of oxygen consumption were measured using intact cells in a high-resolution oxygraph (*Oxygraph-2k; Oroboros Instruments*, Innsbruck, Austria). Oligomycin A (0.5 μg/mL) and FCCP (0.5 μM) were sequentially added to measure the optimal non-coupled respiration and the respiration leak state, respectively. The data were recorded and treated using *DatLab 7* software [15,16,27].

Mitochondrial activity assays

MTT. The parasites were washed twice and incubated in PBS supplemented with 0.1 mM palmitate in 0.35% FFA BSA, 0.35% FFA BSA alone, and 5 mM glucose, and 5 mM histidine or not supplemented media were used as controls (positives and negative, respectively). The cell viability was evaluated at 24 h and 48 h after incubation using the MTT assay, as described in [15,16].

Alamar blue. The parasites were washed twice and incubated in PBS or PBS supplemented with 500 μM ETO in 96-well plates. The plates were maintained at 28˚C during all the experiments. After every 24 h, the cells were incubated with 0.125 $\mu g.mL^{-1}$ of Alamar Blue reagent and kept at 28˚C for 2 h under protection from light. The fluorescence was accessed using the wavelengths λ_{exc} = 530 nm and λ_{em} = 590 nm in the SpectraMax i3 (Molecular Devices) plate reader [17].

Measurement of intracellular ATP content

The intracellular ATP levels were assessed using a luciferase assay kit (Sigma-Aldrich), as described in [15–17]. In brief, the parasites were incubated in PBS supplemented (or not) with 0.1 mM palmitate, 0.35% FFA BSA, 5 mM glucose or 5 mM histidine for 24 h at 28˚C. The ATP concentrations were determined by using a calibration curve with ATP disodium salt (Sigma), and the luminescence at 570 nm was measured as indicated by the manufacturer.

Enzymatic activities

Carnitine palmitoyltransferase 1 (CPT1). The epimastigotes were washed twice in PBS (1,000 x *g*, 5 min at 4˚C), resuspended in buffered Tris-EDTA (100 mM, 2.5 mM and 0.1% Triton X-100) containing 1 μM phenylmethyl-sulphonyl fluoride (PMSF), 0.5 mM N-alpha-p-tosyl-lysyl-chloromethyl ketone (TLCK), 0.01 mg aprotinin and 0.1 mM trans-epoxysuccinyl-L-leucyl amido (4-guanidino) butane (E-64) as a protease inhibitors (Sigma Aldrich) and lysed by sonication (5 pulses for 1 min each, 20%). The lysates were clarified by centrifugation at 10,000 x *g* for 30 min at 4˚C [28]. The soluble fraction was collected and the proteins were quantified by Bradford method [29] and adjusted to 0.1 mg/mL protein. The reaction mixture contained 0.5 mM L-carnitine, 0.1 mM palmitoyl-CoA and 2.5 mM DTNB in Tris-EDTA buffer (pH = 8.0). The CPT1 activity was measured spectrophotometrically at 412 nm by

DTNB reaction with free HS-CoA, forming the TNB^- ion. To calculate the specific activity, the absorbance values were converted into molarity by using the TNB^- extinction molar coefficient of 12,000 $M^{-1}.s^{-1}$ [30]. As a blank, we performed the same assay without adding the substrate. All the enzymatic assays were performed in 96-well plates at a final volume of 0.2 mL in the SpectraMax i3 (Molecular Devices).

Acetyl-CoA carboxylase (ACC). The ACC activity was measured spectrophotometrically by coupling its enzymatic reaction with that of citrate synthase (CS), which uses oxaloacetate and acetyl-CoA to produce citrate. Measurements were performed at the end-points in two steps. First, the reaction mixture contained 100 mM potassium phosphate buffer (pH = 8.0), 15 mM $KHCO_3$, 5 mM $MnCl_2$, 5 mM ATP, 1 mM acetyl-CoA and 0.1 μM biotin. The reaction was initiated by adding 0.1 mg of cell extract and developed using 15 min incubations at 28˚C. The reaction was stopped by adding perchloric acid 40% (v/v) and centrifuged 10,000 x *g* for 15 min at 4˚C. The second reaction was performed by using 0.1 mL of the supernatant from the first reaction, 20 mM oxaloacetate and 0.5 mM of DTNB in 100 mM potassium phosphate buffer (pH = 8.0). The reaction was initiated by adding 0.5 units of CS (Sigma Aldrich). To calculate the specific activity of ACC, we converted the absorbance values to molarity by using the TNB^- extinction molar coefficient of 12,000 $M^{-1}.s^{-1}$. For the blank reaction, we performed the same assay without acetyl-CoA [31].

Hexokinase (HK). The HK activity was measured as described in [32]. Briefly, the activity was measured by coupling the hexokinase activity with a commercial glucose-6-phosphate dehydrogenase, which oxidizes the glucose-6-phosphate (G6PD, SIGMA) resulting from the HK activity with the concomitant reduction of $NADP^+$ to NADPH. The resulting NADPH was spectrophotometrically monitored at 340 nm. The reaction mixture contained 50 mM Triethanolamine buffer pH 7.5, 5 mM $MgCl_2$, 100 mM KCl, 10 mM glucose, 5 mM ATP and 5 U of commercial G6PD. To calculate the specific activity, the absorbance values were converted to molarity using the NADP(H) extinction molar coefficient of 6,220 $M^{-1}.s^{-1}$.

Serine palmitoyltransferase (SPT). The SPT activity was measured through the reduction of the DTNB reaction by the free HS-CoA, forming the TNB^- ion, which was measured spectrophotometrically at 412 nm as previously described [30]. In brief, the epimastigotes were washed twice in PBS, resuspended in Tris-EDTA buffer (100 mM/2.5 mM) containing Triton X-100 0.1% and lysed by sonication (20% of potency, during 2 min). The reaction mixture contained 0.1 mg of protein free-cell extract, 0.5 mM L-serine, 0.1 mM palmitoyl-CoA and 2.5 mM DTNB in Tris-EDTA buffer (100 mM/2.5 mM) pH = 8.0 [33]. To calculate the specific activity, we converted the absorbance values to molarity using the TNB^- extinction molar coefficient of 12,000 $M^{-1}.s^{-1}$. For the blank reaction, we performed the same assay without adding palmitoyl-CoA. All the enzymatic assays were performed in 96-well plates in a final volume of 0.2 mL in the SpectraMax i3 (Molecular Devices).

Glucose and triglyceride quantification

Spent LIT medium from epimastigote cultures was collected by recovering the supernatants from a centrifugation (10,000 x *g* for 15 min at 4˚C). Each sample of spent LIT was analysed for its glucose and triglyceride contents using commercial kits (triglyceride monoreagent and glucose monoreagent by Bioclin Brazil) according to the manufacturer's instructions. These kits are based on colorimetric enzymatic reactions, and the absorbance of each assay was measured in 96-well plates at a final volume of 0.2 mL in the SpectraMax i3 (Molecular Devices).

Proliferation assays

Exponentially growing *T. cruzi* epimastigotes ($5x10^7$ mL^{-1}) were treated with different concentrations of ETO or not treated (negative control) in LIT medium. As a positive control for

growth inhibition, we used a combination of rotenone (60 μM) and antimycin (0.5 μM) [34]. The parasites ($2.5x10^6$ mL^{-1}) were transferred to 96-well plates and then incubated at 28˚C. The cell proliferation was quantified by reading the optical density (OD) at 620 nm for eight days. The OD values were converted to cell numbers using a linear regression equation previously obtained under the same conditions. Each experiment was performed in quadruplicate [35].

Flow cytometry analyses

Cell death. Epimastigotes in the exponential phase of growth were maintained in LIT and treated with ETO 500 μM for 5 days. After the incubation time, the parasites were analysed as described in [35]. The cells were analysed by flow cytometry (FACScalibur BD Biosciences).

Cell cycle (DNA content). Epimastigotes in the exponential phase of growth were maintained in LIT and treated with ETO 500 μM over 5 days. After the incubation time, the parasites were washed twice in PBS and resuspended in lysis buffer (phosphate buffer Na_2HPO_4 7.7 mM; KH_2PO_4 2.3 mM; pH = 7.4) and digitonin 64 μM. After incubating on ice for 30 min, propidium iodide 0.2 μg/mL was added. The samples were analysed by flow cytometry (Guava) adapted from [36].

Fatty acid staining using BODIPY 500/510. Exponentially growing epimastigotes were kept in LIT medium to reach three different cell densities ($2.5x10^7$ mL^{-1}, $5x10^7$ mL^{-1} and 10^8 mL^{-1}) in 24-well plates at 28˚C. Twenty-four hours before the flow cytometry analysis, the parasites were treated with 1 μM C_1-BODIPY 500/510-C_{12}. This fluorophore allows for measurements of the relationship between fatty acid accumulation and consumption by shifting the fluorescence filter. The samples were collected, washed twice in PBS and incubated in 4% paraformaldehyde for 15 min. After incubation, the cells were washed twice with PBS and suspended in the same buffer. Flow cytometry analysis was performed with FL-1 and FL-2 filters in a FACS Fortessa DB. The results were analysed using FlowJo software.

Fluorescence microscopy

The parasites were maintained in LIT medium as previously reported for fatty acid staining using BODIPY 500/510. After incubation, the cells were washed twice in PBS and placed on glass slides. The images were acquired with a digital DFC 365 FX camera coupled to a DMI6000B/AF6000 microscope (Leica). The images were analysed using ImageJ software.

Results

Palmitate supports ATP synthesis in *T. cruzi*

We initially investigated the ability of *T. cruzi* epimastigotes to oxidize fatty acids (for a scheme see Fig 1A). To this end, we used palmitate as a proxy for fatty acids in general. The parasites were incubated with 0.1 mM ^{14}C-[U]-palmitate, which allowed us to measure the production of 1.3 nmoles of CO_2 derived from palmitate oxidation during the first 60 min and 1.5 extra nmoles during the following 60 min (Fig 1B). This finding indicated that beta-oxidation and the further 'burning' of the resulting acetyl-CoA is operative in epimastigote mitochondria. Because palmitate is taken up from extracellular medium and oxidized to CO_2, it is reasonable to assume that it could contribute to resistance to severe nutritional stress. To support this idea, we tested the ability of palmitate to extend parasite survival under extreme nutritional stress. Parasites were incubated for 24 and 48 h in PBS (negative control, in this condition we expected the lower viability after the incubations), 0.1 mM palmitate in PBS supplemented with BSA (as a palmitate carrier), 5.0 mM histidine in PBS or 5.0 mM glucose in PBS (both

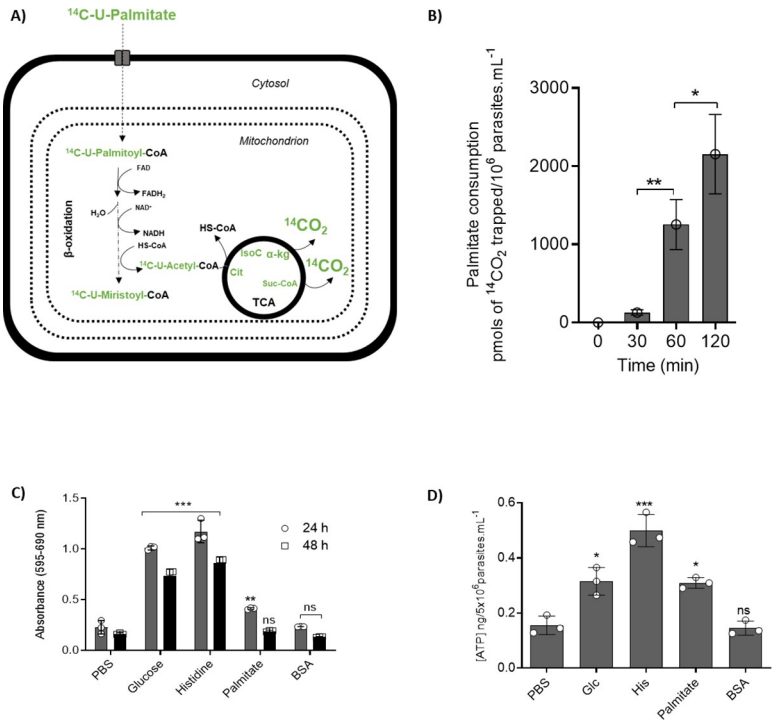

Fig 1. Palmitate oxidation promotes ATP production and viability in epimastigote forms under starvation. A) Schematic representation of ^{14}C-U-palmitate metabolism. The metabolites corresponding to labelled palmitate metabolism are presented in green. B) $^{14}CO_2$ production from epimastigotes incubated in PBS with ^{14}C-U-palmitate 100 μM. The $^{14}CO_2$ was captured at 0, 30, 60 and 120 min. C) Viability of epimastigote forms after incubation with different carbon sources and palmitate. The viability was assessed after 24 and 48 h by MTT assay. D) The intracellular ATP content was evaluated following incubation with different energy substrates or not (PBS, negative control). The ATP concentration was determined by luciferase assay and the data were adjusted by the number of cells. A statistical analysis was performed with one-way ANOVA followed by Tukey's post-test at $p < 0.05$ using the GraphPad Prism 8.0.2 software program. We represent the level of statistical significance in this figure as follows: *** p value < 0.001; ** p value < 0.01; * p value < 0.05. For a p value > 0.05 we consider the differences to be not significant (ns).

https://doi.org/10.1371/journal.ppat.1009495.g001

positive controls, since it is well knowing the ability of both metabolites to extend the parasites ´ viability in metabolic stress conditions, see [15]). As an additional negative control, we used PBS supplemented with BSA without added palmitate. The viability of these cells was assayed by measuring the total reductive activity by MTT assay. Additionally, we measured the total ATP levels. Cells incubated in the presence of palmitate showed higher viability than the negative controls, but not as high as that of parasites incubated with glucose or histidine (Fig 1C). Consistently, parasites incubated in the presence of palmitate showed higher ATP contents than both negative controls. However, the intracellular ATP levels in the cells incubated with palmitate were diminished by half when compared to parasites incubated with histidine. Interestingly, the palmitate kept the ATP content at levels comparable to glucose (Fig 1D).

Epimastigote forms excrete acetate as a primary end-product of palmitate oxidation

Because the epimastigotes were able to oxidize ^{14}C-U-palmitate to $^{14}CO_2$, we were interested in analysing their exometabolome and comparing it with that of parasites exclusively consuming glucose, palmitate or without any carbon source. Thus, we subjected exponentially growing parasites to 16 h of starvation and then incubated them for 6 h in the presence of 0.3 mM palmitate, 10 mM ^{13}C-U-glucose or without any carbon source. For the control, we analysed a

sample of non-starved parasites. After the incubations, the extracellular media were collected and analysed by ^{1}H-NMR spectrometry. As expected, all the incubation conditions produced different flux profiles for excreted metabolites (Figs 2 and S1). Under our experimental conditions, the non-starved parasites primarily excreted succinate and acetate in similar quantities,

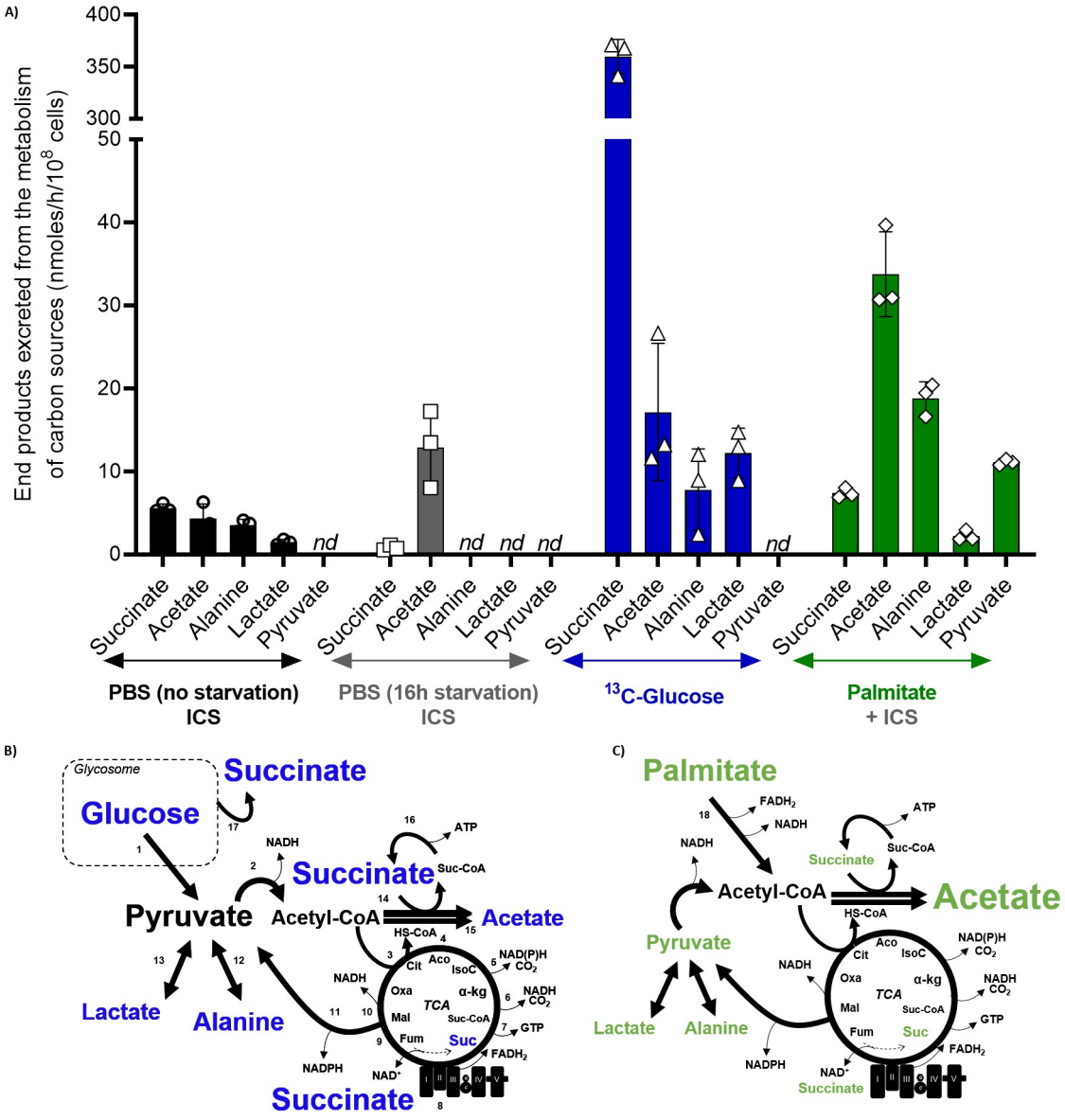

Fig 2. Excreted end products of glucose and palmitate metabolism in epimastigote forms of *T. cruzi*. A) The extracellular medium of epimastigote forms incubated under different conditions was analysed by ^{1}H-NMR spectrometry to detect and quantify the end-products. The resulting data were expressed in nmoles/h/10^{8} cells. Means ± SD of three independent experiments. ICS is internal carbon sources; *nd* is non-detectable. B) and C) Schematic representation of the contribution of glucose and palmitate to the metabolism of epimastigote forms of *T. cruzi*. The glycosomal compartment and TCA cycle are indicated. The amount of end-product determined by the font size. Numbers indicates enzymatic steps. 1. Glycolysis; 2. pyruvate dehydrogenase; 3. citrate synthase; 4. aconitase; 5. isocitrate dehydrogenase; 6. α-ketoglutarate dehydrogenase; 7. succinyl-CoA synthetase; 8. Succinate dehydrogenase/complex II/fumarate reductase NADH-dependent; 9. fumarate hydratase; 10. malate dehydrogenase; 11. Malic enzyme; 12. alanine dehydrogenase/alanine aminotransferase; 13. lactate dehydrogenase; 14. acetate:succinyl-CoA transferase; 15. acetyl-CoA hydrolase; 16. succinyl-CoA synthetase; 17. Glycosomal fumarate reductase and 18. Palmitate oxidation by beta-oxidation, resulting in $FADH_2$, NADH and acetyl-CoA; Abbreviations: Cit: Citrate, Aco: Aconitate, IsoC: Isocitrate, α-kg: α-Ketoglutarate, Suc-CoA: Succinyl-CoA, Suc: Succinate, Fum: Fumarate, Mal: Malate, and Oxa: Oxaloacetate.

https://doi.org/10.1371/journal.ppat.1009495.g002

and alanine and lactate to a lesser extent. Parasites starved for 16 h in PBS and left to incubate in the absence of other metabolites had diminished succinate production (~7-fold) but increased acetate production three-fold compared to the non-starved parasites. It is relevant to stress that the only possible origin for these metabolites are internal carbon sources (ICS). Notably, no other excreted metabolites were detected under these conditions, indicating that under starvation, most of the ICS are transformed into acetate as an end product, which is compatible with the oxidation of internal fatty acids. These results raise the question about the metabolic fates of glucose or fatty acids in previously starved parasites. Starved epimastigotes that recovered in the presence of glucose exhibited a profuse excretion of succinate (450-fold the quantity excreted by the starved cells) and roughly equivalent quantities of acetate compared with the starved cells. Interestingly, lactate and alanine were also excreted at similar levels. As expected, the recovery with glucose produced an increase in all the secreted metabolites. However, analysing their distribution is a reconfiguration of the metabolism towards a majority production of succinate. Finally, in epimastigotes incubated with palmitate, we observed an increase in the acetate and alanine production of approximately 2.5 times to the levels in parasites that recovered in the presence of glucose. Interestingly, succinate is excreted in a smaller quantity than acetate and alanine, but still at 10-fold the rate observed in the starved non-recovered cells. Surprisingly, there was also a significant production of pyruvate (not previously described in the literature, and not observed under any other conditions) and a small amount of lactate derived from palmitate.

Glucose metabolism represses the fatty acid oxidation in epimastigotes

Glucose is the primary carbon source for exponentially proliferating epimastigotes, and after its exhaustion from the culture medium, the parasites change their metabolism to use amino acids as carbon sources preferentially [10]. Therefore, we were interested in analysing if this preference for glucose is maintained in relation to the consumption of lipids. To determine if glucose metabolism interferes with the consumption of fatty acids, we created a 48 h proliferation curve using parasites with an initial concentration adjusted to 2.5 x 10^7 mL^{-1} and quantified them for 24 h each. Under these conditions, the parasites from the beginning of the experiment, at 0 h, are at mid-exponential phase, they are at late exponential phase at 24 h, and at 48 h they reached stationary phase at a concentration of 10 x 10^7 mL^{-1} (Fig 3A). At 0 h, 24 h and 48 h, the culture medium was collected to measure the remaining glucose and triacylglycerol (TAGs) concentrations (Fig 3B and 3C). Most of the glucose was consumed during the first 24 h (during proliferation), while the concentration of TAGs remained the same. After 48 h of proliferation (stationary phase), the TAG levels and lipid contents of the droplets were decreased by 1.5-fold and 2-fold, respectively, suggesting that glucose is preferentially consumed relative to fatty acids. These data show a decrease in the extracellular TAGs between 24 and 48 h, while the glucose was already almost entirely consumed, suggesting that glucose is negatively regulating the fatty acid catabolism.

Epimastigote forms use endogenous fatty acids to support growth after glucose exhaustion

From the previous results, we learned that under glucose deprivation, TAGs are taken up by the epimastigotes, and internally stored fatty acids are mobilized. However, to date, we did not provide any evidence pointing to their use as reduced carbon sources. To confirm this idea, exponentially proliferating epimastigotes were incubated in PBS supplemented with palmitate and ^{14}C-U-glucose, or reciprocally, glucose and ^{14}C-U-palmitate. In both cases, the production of ^{14}C-labelled CO_2 was quantified. The presence of 5 mM glucose diminished the release of

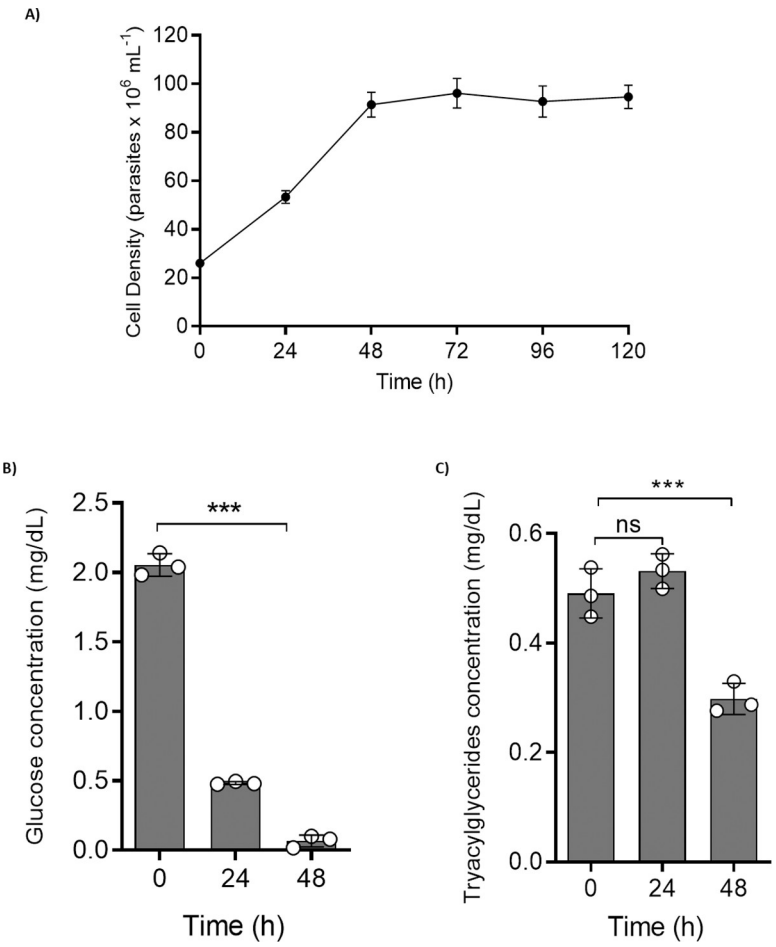

Fig 3. Changes in glucose and triacylglycerol contents in LIT medium. A) Growth curve of epimastigote forms. B) Glucose quantification over 48 h. C) Triacylglycerol levels over 48 h. In each experiment, we collected each medium at different times and subjected it to quantification according to the manufacturer's instructions. All the experiments were performed in triplicates. Statistical analysis was performed with one-way ANOVA followed by Tukey's post-test $p < 0.05$ using the GraphPad Prism 8.0.2 software program. We represent the levels of statistical significance in this figure as follows: *** p value < 0.001; ** p value < 0.01; and * p value < 0.05. For p value > 0.05, we consider the differences not significant (ns).

https://doi.org/10.1371/journal.ppat.1009495.g003

$^{14}CO_2$ from ^{14}C-U-palmitate by 90% while the presence of palmitate did not interfere with the production of $^{14}CO_2$ from ^{14}C-U-glucose (Fig 4). Taken together, our results show that glucose inhibits TAGs and fatty acid consumption, and after glucose exhaustion, a metabolic switch occurs towards the oxidation of internally stored fatty acids.

To monitor the dynamics of use or accumulation of fatty acids in lipid droplets, we used as a probe a fluorescent fatty acid analogue called BODIPY 500/510 C_1-C_{12}. BODIPY shifts its fluorescence from red to green upon the uptake and catabolism of fatty acids, and from green to red when fatty acids are accumulated in the lipid droplets. Parasites collected at the mid and late exponential proliferation phases and the stationary phase were incubated with 1 μM BODIPY 500/510 C_1-C_{12} for 16 h, before fluorescence determination by flow cytometry (Fig 5A, 5B and 5C). The fluorescence values increased with the harvesting time (and therefore, with the glucose depletion), indicating the increased uptake and use of fatty acids as substrates by a fatty acyl-CoA synthetase. These data were confirmed by fluorescence microscopy (Fig 5D). Interestingly, parasites in stationary phase showed an accumulation of activated fatty acids in

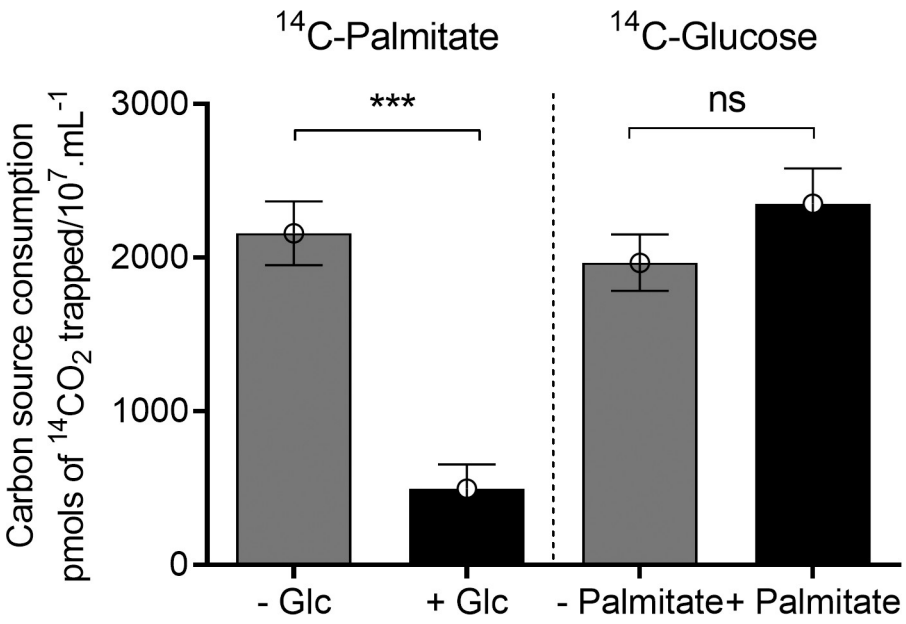

Fig 4. Glucose metabolism inhibits FAO. Parasites were incubated in the presence of ^{14}C-U-palmitate + 5 mM glucose and ^{14}C-U-glucose + 0.1 mM palmitate in PBS. $^{14}CO_2$ production from epimastigotes incubated in PBS. The $^{14}CO_2$ was captured after 120 min of incubation. The experiments were performed in triplicates. Statistical analysis was performed with one-way ANOVA followed by Tukey's post-test $p < 0.05$ using the GraphPad Prism 8.0.2 software program. We represent the level of statistical significance in this figure as follows: *** p value < 0.001; ** p value < 0.01; and * p value < 0.05. For p value > 0.05, we consider the differences not significant (ns).

https://doi.org/10.1371/journal.ppat.1009495.g004

spots along the cell. However, the number of lipid droplets increased upon parasite proliferation (Fig 6A, 6B and 6C). This observation indicates that not only fatty acids metabolism is activated after glucose exhaustion, but also the parasite storage of fatty acids into lipid droplets.

To find if the increase in fatty acid pools is accompanied by a change in the levels of enzymes related to fatty acid metabolism, we evaluated the specific activities of the enzymes hexokinase (HK), which is responsible for the initial step of glycolysis and an indicator of active glycolysis; acetyl-CoA carboxylase (ACC), which produces malonyl-CoA for fatty acid synthesis and carnitine palmitoyltransferase 1 (CPT1), the complex that plays a central role in fatty acid oxidation (FAO) by controlling the entrance of long-chain fatty acids into the mitochondria [37]. For the control, we selected the enzyme serine palmitoyltransferase 1 (SPT1), a constitutively expressed protein in *T. cruzi* [38] (Fig 7). The hexokinase activity diminished up to 30% with the progression of the proliferation curve and the correlated depletion of glucose (Fig 7A). In addition, the ACC activity is no more detectable in the stationary phase cells (Fig 7B). By contrast, the CPT1 activity is increased by ~4-fold when the stationary phase is reached (Fig 7C), which confirms that fatty acid degradation occurs in the absence of glucose. It is noteworthy that the high levels of ACC activity in the presence of glucose supports the idea that under these conditions, fatty acids are probably synthesized instead of being catabolized. As expected, SPT1 did not change during the analysed time frame (Fig 7D).

ETO, a CPT1 inhibitor, affects *T. cruzi* proliferation and mitochondrial activity

To investigate the role of FAO in *T. cruzi*, we tested the effect of a well characterized inhibitor of CPT1, ETO, on the proliferation of epimastigotes. Among the ETO concentrations tested

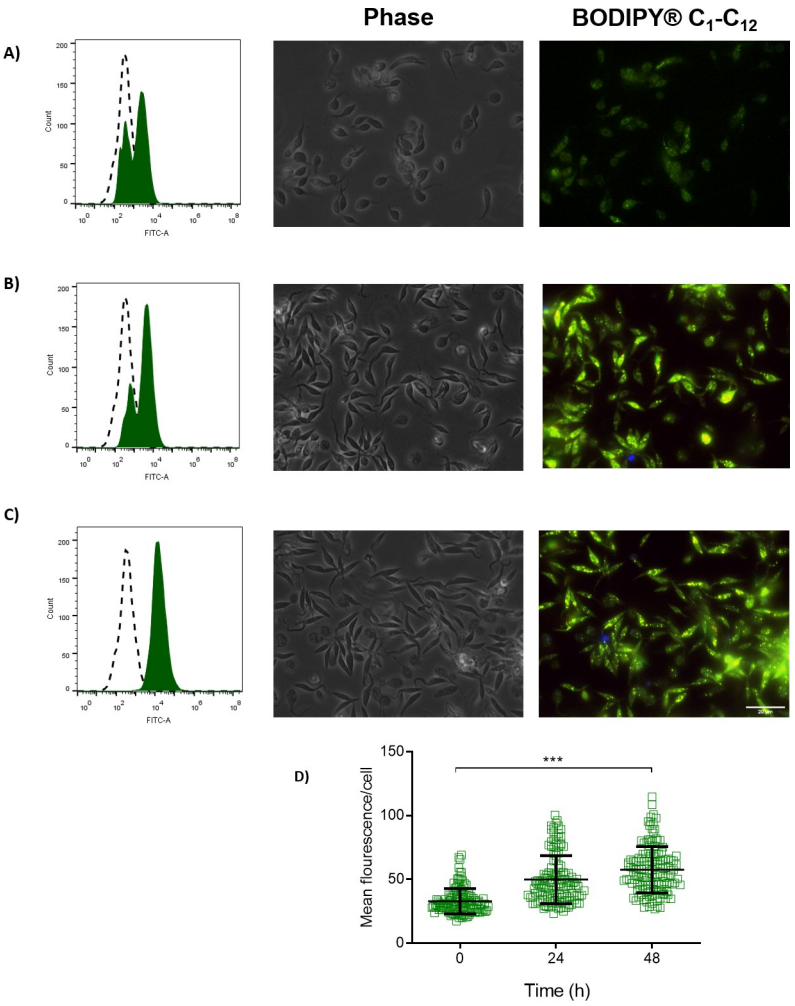

Fig 5. Flow cytometry reveals distinct patterns in fatty acid pools during epimastigote growth. The epimastigotes were treated with 1 μM of BODIPY C_1-C_{12} (500/510) and analysed by flow cytometry and fluorescence microscopy. A) 0 h. B) 24 h. C) 48 h. In the flow cytometry histograms, dashed peaks represent unstained parasites. Green-filled peaks represent stained parasites. D) Mean fluorescence per cell. The fluorescence for each cell was calculated using ImageJ software. All the experiments were performed in triplicates. Statistical analysis was performed with one-way ANOVA followed by Tukey's post-test $p < 0.05$ using the GraphPad Prism 8.0.2 software program. We represent the level of statistical significance in this figure as follows: *** p value < 0.001; ** p value < 0.01; and * p value < 0.05. For p value > 0.05, we consider the differences not significant (ns).

https://doi.org/10.1371/journal.ppat.1009495.g005

here (from 0.1 to 500 μM), only the higher concentration arrested parasite proliferation (Fig 8A). Importantly, the ETO effect was manifested when the parasites reached the late exponential phase (a cell density of approximately $5x10^7$ mL^{-1}). This result is consistent with our previous findings showing that FAO (and thus CPT1 activity) acquires an important role at this point in the proliferation curve. To confirm that CPT1 is in fact a target of ETO in *T. cruzi*, we assayed the drug's effect on the enzyme activity in free cell extracts. Our results showed that 500 μM ETO diminished the CPT1 activity by almost 80% (Fig 8B). To confirm the interference of ETO with the beta-oxidation of fatty acids, parasites incubated in PBS containing ^{14}C-U-palmitate were treated with 500 μM ETO to compare their production of $^{14}CO_2$ with that of the untreated controls. Palmitate-derived CO_2 production diminished by 80% in ETO-treated cells compared to untreated parasites (Fig 8C). In addition, ETO treatment did not

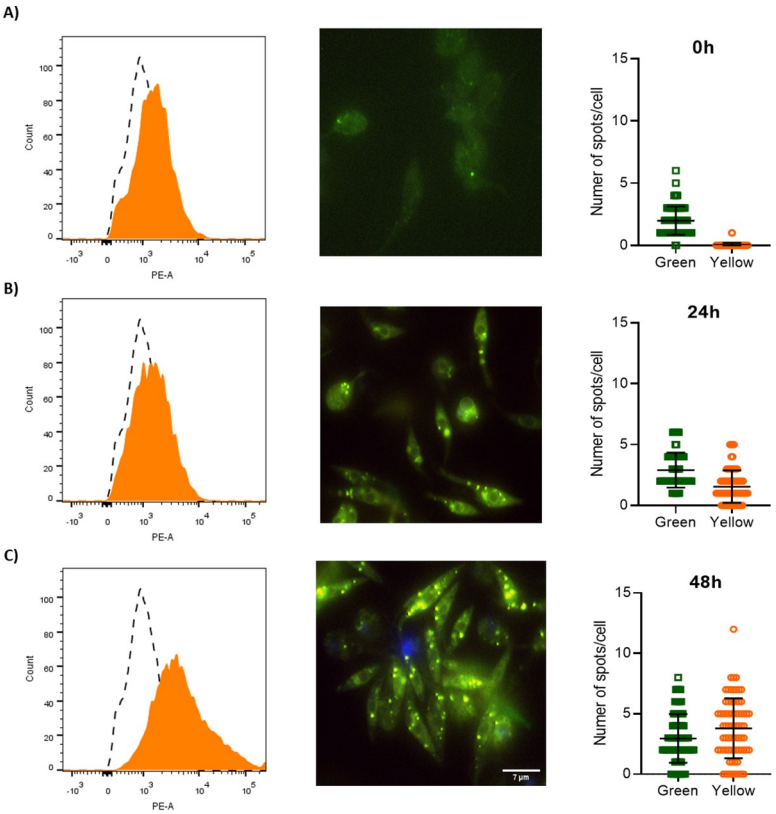

Fig 6. Epimastigote forms accumulates fatty acids into lipid droplets during growth. The epimastigotes were treated with 1 μM BODIPY C_1-C_{12} (500/510) and analysed by flow cytometry and fluorescence microscopy. A) 0 h. B) 24 h. C) 48 h. In the flow cytometry histograms, dashed peaks represent unstained parasites. Yellow filled peaks represent positively stained parasites. The number of green/yellow spots for each cell was calculated using ImageJ software. All the experiments were performed in triplicates.

https://doi.org/10.1371/journal.ppat.1009495.g006

affect the metabolism of ^{14}C-U-glucose or ^{14}C-U-histidine, ruling out a possible unspecific reaction of this drug with CoA-SH as described by [38,39]. Other compounds described as FAO inhibitors were also tested, but none of them inhibited epimastigote proliferation or $^{14}CO_2$ production from ^{14}C-U-palmitate (S3 Fig). In addition, the BODIPY cytometric analysis of cells treated with 500 μM ETO showed a strong decrease in the CoA acylation levels (activation of fatty acids) with respect to the untreated controls (Fig 8D), as confirmed by fluorescence microscopy (Fig 8D). To reinforce the validation of ETO for further experiments, a set of controls are offered in S3 Fig. Our preliminary conclusion is that ETO inhibited beta-oxidation by inhibiting CPT1, confirming that the breakdown of fatty acids is important to proliferation progression in the absence of glucose.

ETO treatment affects cell cycle progression

The metabolic interference of ETO diminished epimastigote proliferation; however, this finding could be due to a decrease in the parasite proliferation rate or an increase in the death rate. Therefore, we checked if this compound could induce cell death through programmed cell death (PCD) or necrosis. PCD is characterized by biochemical and morphological events such as exposure to phosphatidylserine, DNA fragmentation, decreases (or increases) in the ATP levels, and increases in reactive oxygen species (ROS), among others [40]. The parasites were treated with 500 μM of ETO for 5 days, followed by incubation with propidium iodide (PI) for

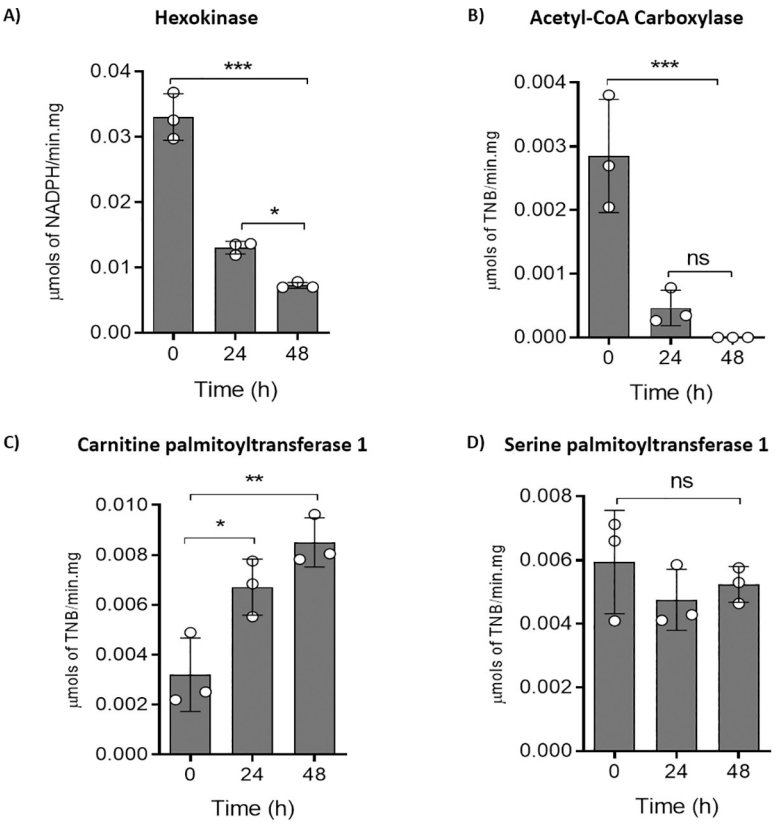

Fig 7. Activities of enzymes related to lipid and glucose metabolism during *T. cruzi* growth curves. A) (HK) Hexokinase B) (ACC) acetyl-CoA carboxylase, C) (CPT1) carnitine-palmitoyltransferase, and D) (SPT) serine palmitoyltransferase. All these activities were measured in crude extracts from epimastigote forms at different moments of the growth curve. All the experiments were performed in triplicates. Time course activities and controls shown in S2 Fig. Statistical analysis was performed with one-way ANOVA followed by Tukey's post-test at $p < 0.05$, using the GraphPad Prism 8.0.2 software program. We represent the level of statistical significance in this figure as follows: *** p value < 0.001; ** p value < 0.01; and * p value < 0.05. For p value > 0.05 we consider the differences not significant (ns).

https://doi.org/10.1371/journal.ppat.1009495.g007

cell membrane integrity analysis and annexin-V FITC to evaluate the phosphatidylserine exposure. Parasites treated with ETO showed negative results for necrosis or programmed cell death markers (Fig 9A), indicating that the cell proliferation was arrested but cell viability was maintained. Because the multiplication rates seemed to be diminished, we performed a cell cycle analysis. Noticeably, the treated parasites were enriched in G1 (85.9%) with respect to non-treated cells (43.6%), suggesting that ETO prevented the entry of epimastigotes into the S phase of the cell cycle (Fig 9B). Last, we noticed that after washing out the ETO, the parasites recovered their proliferation at rates comparable to our untreated controls (Fig 9C).

Inhibition of FAO by ETO affects energy metabolism, impairing the consumption of endogenous fatty acids

The evidence obtained to date suggests that parasites resist metabolic stress by mobilizing and consuming stored fatty acids. Therefore, it is reasonable to hypothesize that ETO, which blocks the mobilization of fatty acids into the mitochondria for oxidation, probably perturbs the O_2 consumption and ATP levels in late-exponential or stationary phase cells. Parasites growing for 5 days under 500 μM ETO treatment or no treatment were collected to evaluate their ability

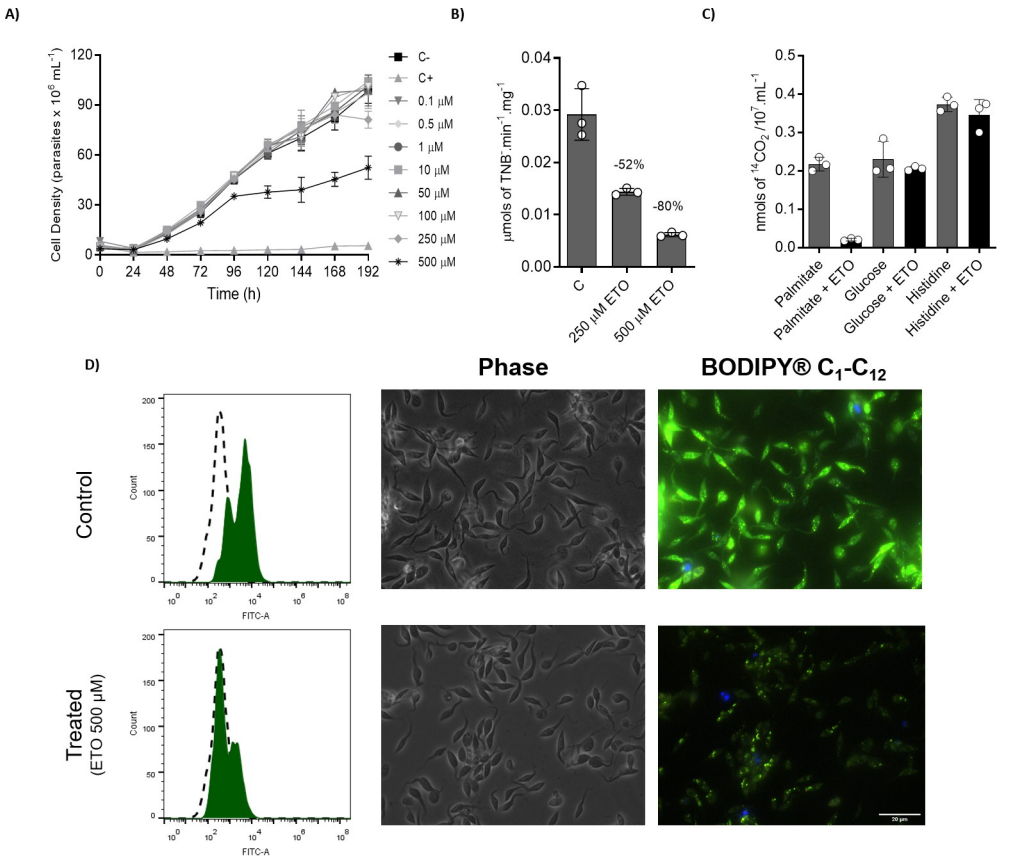

Fig 8. ETO inhibits CPT1 and interferes with cell proliferation in epimastigote forms. (A) Proliferation of epimastigote forms in the presence of 0.1 to 500 μM ETO. For the positive control of dead cells, a combination of antimycin (0.5 μM) and rotenone (60 μM) was used. (B) Inhibition of CPT1 activity in crude extracts using 250 and 500 μM of ETO. C) $^{14}CO_2$ capture from ^{14}C-U-palmitate oxidation. D) Flow cytometry analysis and fluorescence microscopy of epimastigote forms treated (or not) with ETO. In the histograms, dashed peaks represent unstained parasites and green-filled peaks represent parasites stained with BODIPY C_1-C_{12}. All the experiments were performed in triplicates. Statistical analysis was performed with one-way ANOVA followed by Tukey's post-test at $p < 0.05$ using the GraphPad Prism 8.0.2 software program. We represent the level of statistical significance in this figure as follows: *** p value < 0.001; ** p value < 0.01; and * p value < 0.05. For p values > 0.05, we consider the differences not significant (ns).

https://doi.org/10.1371/journal.ppat.1009495.g008

to trigger O_2 consumption (Fig 10A and 10B). The rates of O_2 consumption corresponding to basal respiration were measured in cells resuspended in MCR respiration buffer. We then measured the leak respiration by inhibiting the ATP synthase with oligomycin A. Finally, to measure the maximum capacity of the electron transport system (ETS), we used the uncoupler FCCP [27]. Our results demonstrate that compared to no treatment, ETO treatment diminishes the rate of basal O_2 consumption, the leak respiration and the ETS capacity (Fig 10C). In general, respiratory rates diminished in parasites treated with ETO when compared to the untreated ones. As expected, ETO treatment led to a 75% decrease in the levels of total intracellular ATP compared to untreated parasites (Fig 10D). To complement this result, because all these experiments were conducted in the complete absence of an oxidizable external metabolite, our results show that the parasite is able to oxidize internal metabolites (Fig 10A and 10B). Taking into account that treating parasites with ETO diminished the basal respiration rates of these parasites by approximately one-half (Fig 10A and 10B), it is reasonable to conclude that a relevant part of the respiration in the absence of external oxidisable metabolites is based on the

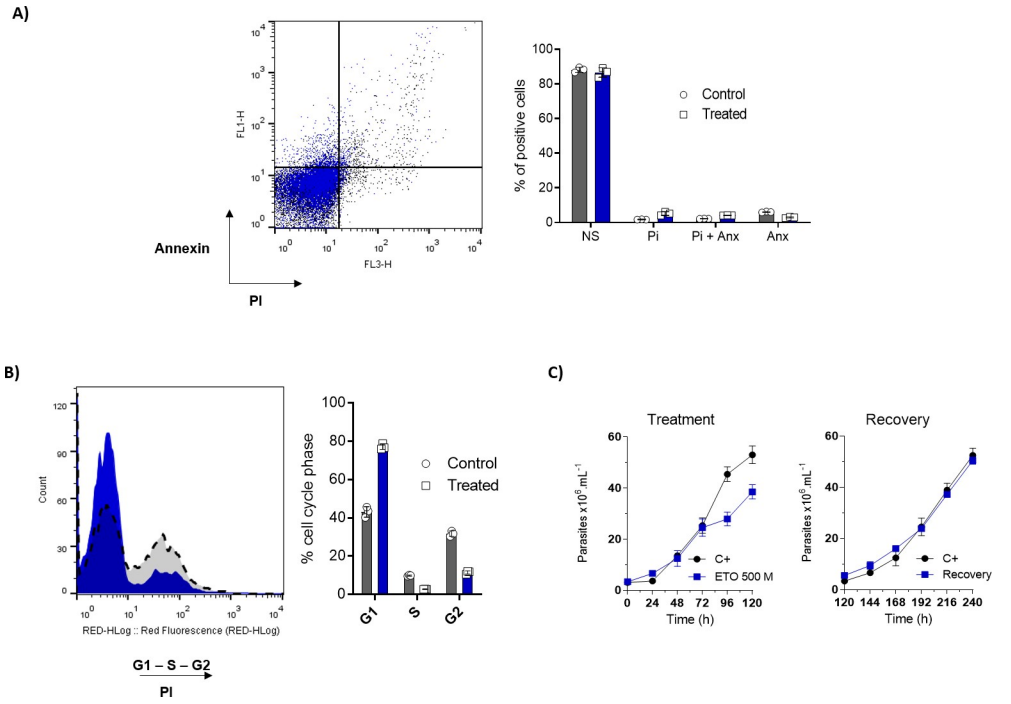

Fig 9. Analysis of extracellular phosphatidylserine exposure, membrane integrity and cell cycle after ETO treatment. Parasites in the exponential growth phase were treated with 500 μM of ETO for 5 days. (A) Following the incubation period, the parasites were labelled with propidium iodide (PI) and annexin V-FITC (ANX) and analysed by flow cytometry. (B) The cell cycle was assessed using PI staining. (C) Growth curves of epimastigote forms before and after removing the treatment. All the experiments were performed in triplicates. Statistical analysis was performed with one-way ANOVA followed by Tukey's post-test $p < 0.05$, using the GraphPad Prism 8.0.2 software program. We represent the level of statistical significance in this figure as follows: *** p value < 0.001; ** p value < 0.01; and * p value < 0.05. For p values > 0.05, we consider the differences not significant (ns).

https://doi.org/10.1371/journal.ppat.1009495.g009

consumption of internal lipids. This is consistent with the confirmation that epimastigotes maintain their viability in the presence of non-fatty acid carbon sources in the presence of ETO (S4 Fig). In summary, these results confirm that ETO is interfering with ATP synthesis through oxidative phosphorylation in epimastigote forms.

Endogenous fatty acids contribute to long-term starvation resistance in epimastigote forms

As previously demonstrated, ETO interferes with the consumption of endogenous fatty acids, and this impairment causes ATP depletion and cell cycle arrest. One intriguing characteristic of the insect stages of *T. cruzi* is their resistance to starvation. To observe the importance of internal fatty acids in this process, we incubated epimastigotes in PBS in the presence (or absence) of 500 μM ETO. The mitochondrial activity of these cells was followed for 24 h with Alamar Blue. Our results showed that the mitochondrial activity of the parasites in the presence of ETO was reduced by 31% after 48 h of starvation, and 65% after 72 h of starvation (Fig 11) compared to the controls (untreated parasites). These data confirmed our hypothesis that the breakdown of accumulated fatty acids partially contributes to the resistance of the parasite under severe starvation.

Inhibition of CPT1 impairs metacyclogenesis

Considering that the FAO increases in the epimastigotes during the stationary phase, and that differentiation into infective metacyclic trypomastigotes (metacyclogenesis) is triggered in the

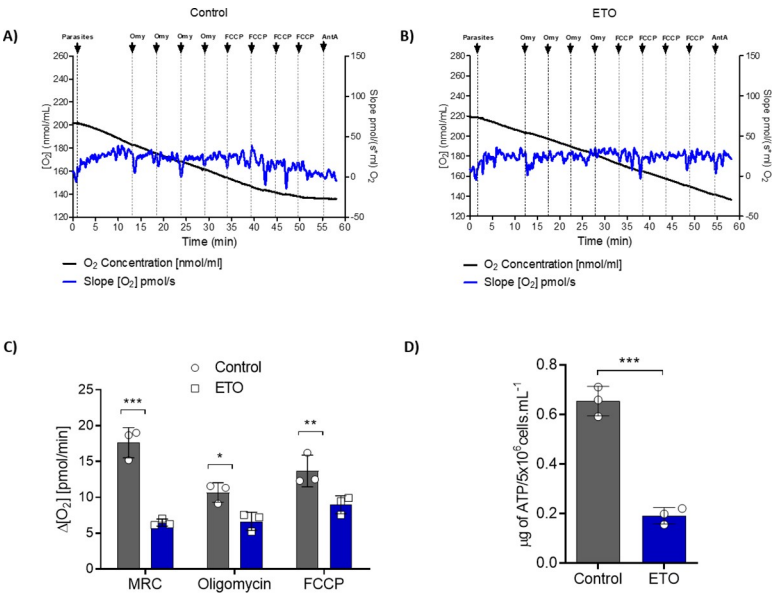

Fig 10. Effects of ETO on respiration and ATP production in epimastigote forms of *T. cruzi*. (A) Oxygen consumption of epimastigote forms after normal growth in LIT medium. (B) Oxygen consumption after ETO 500 μM treatment. Parasite growth in LIT medium with the compound until the 5th day. In black, a time-course register of the concentration (pmols) of O_2 in the respiration chamber. In blue, negative of the concentration derivative (pmols) of O_2 with respect to time (velocity of O_2 consumption in pmoles per second). The parasites were washed twice in PBS and kept in MRC buffer at 28˚C during the assays. (C) The basal respiration (initial oxygen flux values, MRC), respiration leak after the sequential addition of 0.5 μg/mL of oligomycin A (2 μg/mL), and electron transfer system (ETS) capacity after the sequential addition of 0.5 μM FCCP (2 μM) were measured for each condition. (D) Intracellular levels of ATP after treating with 500 μM ETO. The intracellular ATP content was assessed following incubation with different energy substrates or not (PBS, negative control). The ATP concentration was determined by luciferase assay and the data were adjusted by the number of cells. All the experiments were performed in triplicates. Statistical analysis was performed with one-way ANOVA followed by Tukey's post-test at $p < 0.05$ using GraphPad Prism 8.0.2 software. We represent the level of statistical significance as follows: *** p value < 0.001; ** p value < 0.01; and * p value < 0.05. For p values > 0.05, we consider the differences not significant (ns).

https://doi.org/10.1371/journal.ppat.1009495.g010

stationary phase of epimastigote parasites, one might expect a possible relationship between the consumption of fatty acids and metacyclogenesis. To approach this possibility, we initially compared the CPT1 activity of stationary epimastigote forms before and after a 24 h incubation in the differentiation medium TAU-3AAG. As observed, there is an increase in CPT1 activity after submitting the parasites to the metacyclogenesis *in vitro* (Fig 12A). Parasites were then submitted to differentiation with TAU-3AAG medium in the presence of the probe BODIPY. The probe was incorporated into lipid droplets, confirming that fatty acids metabolism was active during the beginning of metacyclogenesis (Fig 12B). To address the importance of FAO during differentiation, metacyclogenesis was induced *in vitro* on ETO-treated or untreated (control) parasites. ETO treatment interfered with differentiation, diminishing the number of metacyclic forms present in the culture (Fig 12C). In addition, this inhibition was dose-dependent, with an $IC_{50} = \pm 32.96$ μM (Fig 12D). Importantly, we ruled out that the variation found in the differentiation rates was due to a selective death of treated epimastigotes, since their survival during this experiment in the presence or absence of ETO (from 5 to 500 μM) was not significantly different (S5 Fig). Based on these data, we could conclude that fatty acid oxidation, at the level of the CPT1, was also participating in the regulation of metacyclogenesis.

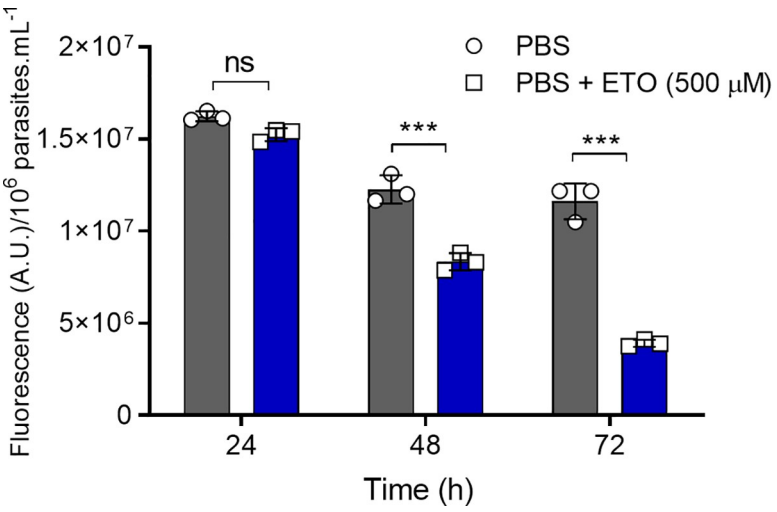

Fig 11. Internal fatty acid consumption contributes to parasite viability under severe nutritional starvation. Viability of epimastigote forms after incubation in PBS with or without ETO. The viability was assessed every 24 h using Alamar Blue. Statistical analysis was performed with one-way ANOVA followed by Tukey's post-test $p < 0.05$ using GraphPad Prism 8.0.2 software. We represent the levels of statistical significance as follow: *** p value < 0.001, and for p values > 0.05, we consider the differences not significant (ns).

https://doi.org/10.1371/journal.ppat.1009495.g011

Discussion

During the journey of *T. cruzi* inside the insect vector, the glucose levels decrease rapidly after each blood meal [41], leaving the parasite exposed to an environment rich in amino and fatty

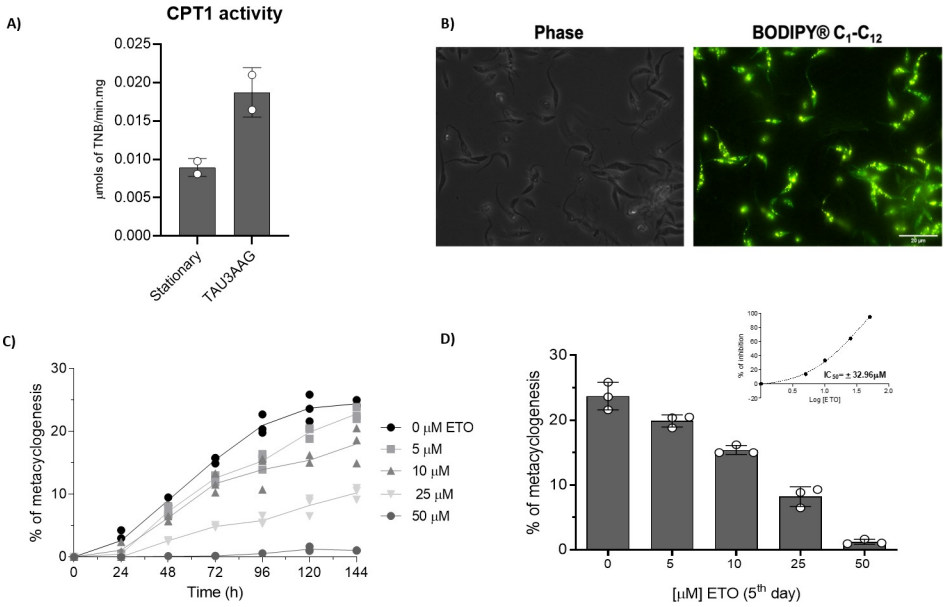

Fig 12. ETO inhibits metacyclogenesis. A) CPT1 activity of epimastigote forms in stationary phase and 24h after incubated in TAU-3AAG medium (for triggering metacyclogenesis). B) Fluorescence microscopy of cells incubated in TAU-3AAG in the presence of BODIPY 500–510 C_1-C_{12}. C) Effects of different ETO concentrations on metacyclogenesis. The differentiation was evaluated by counting the cells in a Neubauer chamber each day for 6 days. This experiment was performed in triplicate. D) Percentage of differentiation at the 5th day of differentiation. Inset: IC_{50} of metacyclogenesis inhibition by ETO. The enzymatic activities were measured in duplicate. All the other experiments were performed in triplicates.

https://doi.org/10.1371/journal.ppat.1009495.g012

acids in the digestive tube of *Rhodnius prolixus* [42,43]. Because the digestive tract of triatomine insects possesses a perimicrovillar membrane, which is composed primarily of lipids and is enriched by glycoproteins [44], it has been speculated that its degradation could provide lipids for parasite metabolism [45]. In this study, we showed that the insect stages of *T. cruzi* coordinate the activation of fatty acid consumption with the metabolism of glucose. Our experiments corroborate early studies about the relatively slow use of palmitate as an energy source by proliferating epimastigotes [46,47]. In addition, our results shed light on the end product excretion by epimastigote forms during incubation under starvation conditions, and during their recovery from starvation using glucose or palmitate. First, we showed that non-starved and starved parasites recovered in the presence of glucose, excreting succinate as their primary metabolic waste, as expected [48,49]. After 16 h of nutritional starvation, the consumption of internal carbon sources produces acetate as the primary end-product. In the presence of glucose after 16 h of starvation, we found that glucose-derived carbons contribute to the excreted pools of acetate and lactate. Interestingly, palmitate metabolism contributed to the increase in acetate production, followed by the production of alanine, pyruvate, succinate and lactate. The unexpected production of alanine, pyruvate and lactate can be explained by an increase in the TCA cycle activity, producing malate, which can be converted into pyruvate by the decarboxylative reaction of the malic enzyme (ME) [50]. Pyruvate can be converted into alanine through a transamination reaction by an alanine- [51], a tyrosine- [52] an aspartate aminotransferase [53], or a reductive amination by an alanine dehydrogenase [54]. The excretion of lactate could be a consequence of lactate dehydrogenase activity. However, it should be noted that this enzymatic activity has not been observed to date. In relation to the succinate production, a relevant factor favouring this process is the production of NADH by the third step of the beta-oxidation (3-hydroxyacyl-CoA dehydrogenase). This NADH can be oxidized through the activity of NADH-dependent mitochondrial fumarate reductase [55], which concomitantly converts NADH into NAD^+ and fumarate into succinate. This succinate can be excreted or re-used by the TCA cycle, and the resulting NAD^+ can be used as a cofactor for other enzymes.

As previously mentioned, it is well known that during the initial phase of proliferation, epimastigotes preferentially consume glucose, and during the stationary phase, a metabolic switch occurs towards the consumption of amino acids [8,10,56]. Our results show that this switch constitutes a broader and more systemic metabolic reprogramming, which also includes FAO. We detected this switch through changes in the enzymatic activities of key enzymes responsible for the regulation of FAO, such as CPT1 and ACC, which have increased and decreased activities, respectively, in the presence of glucose. Our findings showed that the inhibition of CPT1 affects the late phase of proliferation of epimastigotes when the switch to FAO has already occurred.

An interesting question about *T. cruzi* epimastigotes is how they survive long periods of starvation. Early data showed high respiration levels in epimastigotes incubated in the absence of external oxidisable carbon sources. This oxygen consumption was attributed to the breakdown of TAGs into free fatty acids and their further oxidation [57]. Here, we confirmed this finding by inhibiting the internal fatty acid consumption, which in turn diminished the oxidative phosphorylation activity, internal ATP levels and the total reductive activity of parasites under severe nutritional stress. Even more notably, we showed that under these conditions, the lipids stored in lipid droplets [58,59] are consumed. Unlike what has been observed in procyclic forms of *T. brucei*, in which the function of lipid droplets is not clear [60], our results show that in *T. cruzi*, they are committed to epimastigote survival under extreme metabolic stress. Of course, the contribution of other metabolic sources and processes such as autophagy in coping with nutritional stress cannot be ruled out [61].

Multiple metabolic factors have been involved in metacyclogenesis, such as the proline, aspartate, glutamate [62], glutamine [17] and lipids present in the triatomine digestive tract [63]. Interestingly, the occurrence of metacyclic trypomastigotes in culture leads to an increase in CO_2 production from labelled palmitate [47]. The ETO treatment inhibited metacyclogenesis *in vitro*, showing that the consumption of internal fatty acids is important for cell differentiation. Consequently, we propose that lipids are not only external signals of metacyclogenesis, as previously suggested [63], but they also have a central role in the bioenergetics of metacyclogenesis. It was previously described that this differentiation process is triggered by a starvation followed by the addition of energy and carbon sources such as a combination of glucose, proline, aspartate and glutamate [64], just proline [65], or just glutamine [17] must be supplied. In our experiment, we added the carbon and energy sources alone, or in combination with ETO, which allowed us to dissect the effect of lipids mobilization into the mitochondria after the starvation. Our results indicate that, in addition to the oxidation of several metabolites (glucose and amino acids), the mitochondrial metabolism of lipids, and probably the reduced cofactors resulting from these processes are contributing to the mitochondrial ATP production necessary to support this differentiation step. Summarizing, this observation points to the participation of lipids metabolism in *T*. *cruzi* metacyclogenesis.

In conclusion, fatty acids are important carbon sources for *T*. *cruzi* epimastigotes in the absence of glucose. The completeness and function of the TCA cycle in trypanosomatids have been a matter of controverse [66–68]. However, several works have shown in *T*. *cruzi* the functionality of TCA cycle and more recently, most of the TCA cycle intermediates has been detected by metabolomic analysis [10]. In addition, Villafraz et al demonstrated that even in procyclics of *T*. *brucei* the TCA cycle is complete and works in the oxidative direction [69]. Therefore, we propose that palmitate can be taken up by the cells and fuel the TCA cycle by producing acetyl-CoA, the oxidation of which generates CO_2. However, in the absence of external carbon sources, lipid droplets become the primary sources of fatty acids, helping the organism to survive nutritional stress. Importantly, FAO supports endogenous respiration rates and ATP production and powers metacyclogenesis.

Supporting information

S1 Fig. ^{1}H-NMR analysis of excreted end products from glucose and threonine metabolism. The metabolic end products (succinate, acetate, alanine and lactate) excreted by the epimastigote cells that were incubated after 6 h in PBS (A), PBS after 16 h of starvation without (B) or with D-[U-^{13}C]-glucose (C) or palmitate (D) were determined by ^{1}H-NMR. Each spectrum corresponds to one representative experiment from a set of at least 3. A part of each spectrum ranging from 0.5 ppm to 4 ppm is shown. The resonances were assigned as indicated: A_{12}, acetate; A_{13}, ^{13}C-enriched acetate; Al_{12}, alanine; Al_{13}, ^{13}C-enriched alanine; G_{13}, ^{13}C-enriched glucose; L_{12}, lactate; L_{13}, ^{13}C-enriched lactate; P_{12}, palmitate; S_{12}, succinate; and S_{13}, ^{13}C-enriched succinate.
(TIF)

S2 Fig. Time course activities of enzymes measured in this work. A) (ACC) acetyl-CoA carboxylase, B) (CPT1) carnitine-palmitoyltransferase, and C) (SPT) serine palmitoyltransferase. All the activities were measured in cell-free extracts of epimastigote forms at different moments of the growth curve as indicated in the main text. All the measurements were performed in triplicates.
(TIF)

S3 Fig. Other FAO inhibitors did not affect cell proliferation and FAO in the epimastigote forms. Well-known FAO inhibitors such as valproic acid [57], trimetazidine [58,59] and β-hydroxybutyrate [60], were assayed for their effect on the proliferation of *T*. *cruzi* epimastigotes. None of the compounds at the tested concentrations inhibit the epimastigotes proliferation. We used the compounds at the higher concentration tested for epimastigotes proliferation to assay their ability to inhibit FAO by $^{14}CO_2$ trapping using U-^{14}C-palmitate as a substrate. As observed, none of these compound inhibited the $^{14}CO_2$ production from palmitate, confirming that they are not inhibiting FAO in *T*. *cruzi*. The compounds were assayed at concentrations between 0.1 and 1000 μM. For positive controls of dead cells, a combination of antimycin (0.5 μM) and rotenone (60 μM) were used. The maximum concentration tested for these compounds does not diminish CO_2 liberation from FAO. A) Valproic Acid (AV). B) Trimetazidine (TMZ). C) β-hydroxybutyrate (βHOB).
(TIF)

S4 Fig. ETO affected specifically FAO and did not affect the viability of epimastigote forms in the presence of other carbon sources. To confirm that ETO is acting on FAO and to rule out that our findings are due to off-target effects that can happenas at concentrations of up to 200 μM [61,62] we assayed its effect in the presence of non-lipidic carbon sources. The parasites were incubated for 24 h in PBS (negative control), 0.1 mM palmitate supplemented with BSA, 5.0 mM histidine, 5 mM glucose, 0.1 mM carnitine and BSA without adding palmitate in the presence (or not) of 500 μM ETO. As expected, ETO treatment did not affect the viability of cells incubated in glucose or histidine but did affect the viability of the cells incubated with palmitate or carnitine. Surprisingly, we also observed an ETO effect on parasites under metabolic stress, such as those incubated with PBS or BSA. This finding could be explained by the fact that under metabolic stress, the parasite mobilizes and consumes its internal lipids. The viability of these cells was inferred from by measuring the total reductive activity using MTT assays after 24 h.
(TIF)

S5 Fig. Viability of epimastigote forms subjected to metacyclogenesis under different ETO concentrations. We assassed the viability of parasites during metacyclogenesis in the presence or not of ETO. Stationary epimastigotes in TAU-3AAG media were treated with different concentrations of ETO (5 to 500 μM for 24 hs, panel A, or 5 to 50 μM for 120 h, panel B). The viability of these cells was inferred by measuring the total reductive activity using an Alamar blue assay [63]. In addition, the parasites were maintained during metacyclogenesis in the presence of 50 μM ETO (or not, control) and differentiation was followed up by daily counts, based on the percentage of metacyclic trypomastigotes collected in culture supernatant (panel C). Considering that TAU-3AAG contains glucose in its composition, we performed an *in vitro* metacyclogenesis using only proline as a metabolic inducer [64]. As observed, even in the absence of glucose, ETO treatment affects metacyclogenesis.
(TIF)

Acknowledgments

We thank the Core Facility for Scientific Research at the University of Sao Paulo (CEFAP-USP/FLUIR) for the flow cytometry analysis and Dr. Mauro Javier Veliz Cortez (Department of Parasitology, ICB-USP) for the microscopy support.

Author Contributions

Conceptualization: Rodolpho Ornitz Oliveira Souza, Rui Curi, Frédéric Bringaud, Ariel Mariano Silber.

Data curation: Rodolpho Ornitz Oliveira Souza, Flávia Silva Damasceno, Sabrina Marsiccobetre, Marc Biran, Frédéric Bringaud, Ariel Mariano Silber.

Formal analysis: Rodolpho Ornitz Oliveira Souza, Flávia Silva Damasceno, Marc Biran, Gilson Murata, Frédéric Bringaud, Ariel Mariano Silber.

Funding acquisition: Frédéric Bringaud, Ariel Mariano Silber.

Investigation: Rodolpho Ornitz Oliveira Souza, Flávia Silva Damasceno, Sabrina Marsiccobetre, Gilson Murata, Ariel Mariano Silber.

Methodology: Rodolpho Ornitz Oliveira Souza, Flávia Silva Damasceno, Sabrina Marsiccobetre, Marc Biran, Frédéric Bringaud.

Project administration: Ariel Mariano Silber.

Resources: Frédéric Bringaud, Ariel Mariano Silber.

Supervision: Rui Curi, Frédéric Bringaud, Ariel Mariano Silber.

Validation: Flávia Silva Damasceno, Rui Curi, Ariel Mariano Silber.

Visualization: Frédéric Bringaud.

Writing – original draft: Rodolpho Ornitz Oliveira Souza, Ariel Mariano Silber.

Writing – review & editing: Frédéric Bringaud, Ariel Mariano Silber.

References

1. WHO (last visit on March, 2021) Chagas disease (American trypanosomiasis). WHO https://www.who.int/health-topics/chagas-disease.
2. Perez-Molina JA, Molina I (2018) Chagas disease. Lancet. 391: 82–94. https://doi.org/10.1016/S0140-6736(17)31612-4 PMID: 28673423
3. Melo RdFP, Guarneri AA, Silber AM. The influence of environmental cues on the development of *Trypanosoma cruzi* in triatominae vector. 2020; Front Cell Infect Microbiol 10: 27–27. https://doi.org/10.3389/fcimb.2020.00027 PMID: 32154185
4. Lisvane Silva P, Mantilla BS, Barison MJ, Wrenger C, Silber AM. The uniqueness of the *Trypanosoma cruzi* mitochondrion: opportunities to identify new drug target for the treatment of Chagas disease. Curr Pharm Des. 2011; 17: 2074–2099. https://doi.org/10.2174/138161211796904786 PMID: 21718252
5. Bern C. Chagas' Disease. N Engl J Med. 2015; 373: 1882.
6. De Souza W. Basic cell biology of *Trypanosoma cruzi*. Curr Pharm Des. 2002; 8: 269–285. https://doi.org/10.2174/1381612023396276 PMID: 11860366
7. Li Y, Shah-Simpson S, Okrah K, Belew AT, Choi J, Caradonna KLet al. Transcriptome remodeling in *Trypanosoma cruzi* and human cells during intracellular infection. PLOS Pathog. 2016; 12: e1005511–e1005511. https://doi.org/10.1371/journal.ppat.1005511 PMID: 27046031
8. Marchese L, Nascimento J, Damasceno F, Bringaud F, Michels P, Silber AM. The uptake and metabolism of amino acids, and their unique role in the biology of pathogenic trypanosomatids. Pathogens. 2018; 7: 36–36.
9. Cazzulo JJ. Energy metabolism in *Trypanosoma cruzi*. Subcell Biochem. 1992; 18: 235–257. https://doi.org/10.1007/978-1-4899-1651-8_7 PMID: 1485353
10. Barison MJ, Rapado LN, Merino EF, Furusho Pral EM, Mantilla BS, Marchese Let al. Metabolomic profiling reveals a finely tuned, starvation-induced metabolic switch in *Trypanosoma cruzi* epimastigotes. J Biol Chem. 2017; 292: 8964–8977. https://doi.org/10.1074/jbc.M117.778522 PMID: 28356355
11. Zeledon R. Comparative physiological studies on four species of hemoflagellates in culture. II. Effect of carbohydrates and related substances and some amino compounds on the respiration. J. Parasitol. 1960; 46: 541–541. PMID: 13788134
12. Sylvester D, Krassner SM. Proline metabolism in *Trypanosoma cruzi* epimastigotes. Comp Biochem Physiol B: Comp. Biochem. 1976; 55: 443–447. https://doi.org/10.1016/0305-0491(76)90318-7 PMID: 789007

13. Paes LS, Suarez Mantilla B, Zimbres FM, Pral EM, Diogo de Melo P, Tahara EBet al. Proline dehydrogenase regulates redox state and respiratory metabolism in *Trypanosoma cruzi*. PLoS ONE. 2013; 8: e69419–e69419. https://doi.org/10.1371/journal.pone.0069419 PMID: 23894476

14. Mantilla BS, Paes LS, Pral EMF, Martil DE, Thiemann OH, Fernández-Silva P et al. Role of Δ1-pyrroline-5-carboxylate dehydrogenase supports mitochondrial metabolism and host-cell invasion of *Trypanosoma cruzi*. J Biol Chem. 2015; 290: 7767–7790. https://doi.org/10.1074/jbc.M114.574525 PMID: 25623067

15. Barisón MJ, Damasceno FS, Mantilla BS, Silber AM. The active transport of histidine and its role in ATP production in *Trypanosoma cruzi*. J Bioenerg Biomembr. 2016; 48: 437–449. https://doi.org/10.1007/s10863-016-9665-9 PMID: 27222029

16. Girard RMBM, Crispim M, Alencar MB, Silber AM. Uptake of L-alanine and its distinct roles in the bioenergetics of *Trypanosoma cruzi*. 2018; mSphere 3: e00338–18. https://doi.org/10.1128/mSphereDirect.00338-18 PMID: 30021880

17. Damasceno FS, Barisón MJ, Crispim M, Souza ROO, Marchese L, Silber AM. L-Glutamine uptake is developmentally regulated and is involved in metacyclogenesis in *Trypanosoma cruzi*. Mol Biochem Parasitol. 2018; 224:17–25. https://doi.org/10.1016/j.molbiopara.2018.07.007 PMID: 30030130

18. Gualdrón-López M, Brennand A, Hannaert V, Quiñones W, Cáceres AJ, Bringaud F, et al. When, how and why glycolysis became compartmentalised in the Kinetoplastea. A new look at an ancient organelle. Int J Parasitol. 2012; 42: 1–20. https://doi.org/10.1016/j.ijpara.2011.10.007 PMID: 22142562

19. Gabaldón T, Ginger ML, Michels PA. Peroxisomes in parasitic protists. Mol Biochem Parasitol. 2016; 209: 35–45. https://doi.org/10.1016/j.molbiopara.2016.02.005 PMID: 26896770

20. Gualdron-López M, Vapola MH, Miinalainen IJ, Hiltunen JK, Michels PA, Antonenkov VD. Channel-forming activities in the glycosomal fraction from the bloodstream form of *Trypanosoma brucei*. PLoS One. 2012; 7: e34530. https://doi.org/10.1371/journal.pone.0034530 PMID: 22506025

21. Bakker BM, Mensonides FI, Teusink B, van Hoek P, Michels PA, Westerhoff HV. Compartmentation protects trypanosomes from the dangerous design of glycolysis. Proc Natl Acad Sci U S A. 2000; 97: 2087–2092. https://doi.org/10.1073/pnas.030539197 PMID: 10681445

22. Quiñones W, Acosta H, Gonçalves CS, Motta MCM, Gualdrón-López M, Michels PA. Structure, properties, and function of glycosomes in *Trypanosoma cruzi*. Front Cell Infect Microbiol. 2020; 10: 25. https://doi.org/10.3389/fcimb.2020.00025 PMID: 32083023

23. Acosta H, Dubourdieu M, Quiñones W, Cáceres A, Bringaud F, Concepción JL. Pyruvate phosphate dikinase and pyrophosphate metabolism in the glycosome of *Trypanosoma cruzi* epimastigotes. Comp Biochem Physiology B: Biochem Mol Biol. 2004; 38: 347–356. https://doi.org/10.1016/j.cbpc.2004.04.017 PMID: 15325334

24. Acosta H, Burchmore R, Naula C, Gualdrón-López M, Quintero-Troconis E, Cáceres AJ, et al. Proteomic analysis of glycosomes from *Trypanosoma cruzi* epimastigotes. Mol Biochem Parasitol. 2019; 229: 62–74. https://doi.org/10.1016/j.molbiopara.2019.02.008 PMID: 30831156

25. Camargo EP. Growth and differentiation in *Trypanosoma cruzi*. I. Origin of metacyclic trypanosomes in liquid media. Rev Inst Med Trop Sao Paulo. 1964; 6: 93–100. PMID: 14177814

26. Huynh FK, Green MF, Koves TR, Hirschey MD. Measurement of fatty acid oxidation rates in animal tissues and cell lines. Meth Enzymol. 2014; 542: 391–405. https://doi.org/10.1016/B978-0-12-416618-9.00020-0 PMID: 24862277

27. Alencar MB, Girard RBMM, Silber AM. Measurement of energy states of the trypanosomatid mitochondrion. Meth Mol Biology (Clifton, NJ). 2020; 2116: 655–671. https://doi.org/10.1007/978-1-0716-0294-2_39 PMID: 32221948

28. Marchese L, Olavarria K, Mantilla BS, Avila CC, Souza ROO, Damasceno FS, et al. *Trypanosoma cruzi* synthesizes proline via a Δ1-pyrroline-5-carboxylate reductase whose activity is fine-tuned by NADPH cytosolic pools. Biochem J. 2020; 477: 1827–1845. https://doi.org/10.1042/BCJ20200232 PMID: 32315030

29. Bradford MM. A rapid and sensitive method for the quantitation of microgram quantities of protein utilizing the principle of protein-dye binding. Anal Biochem. 1976; 72: 248–254. https://doi.org/10.1006/abio.1976.9999 PMID: 942051

30. Bieber PLL, Abraham T, Helmrath T, Kim Y, Dehlin R. A rapid spectrophotometric assay for carnitine palmitoyltransferase. Anal Biochem. 1972; 50: 509–518 https://doi.org/10.1016/0003-2697(72)90061-9 PMID: 4630394

31. Willis LB, Saridah W, Omar W, Ravigadevi S, Sinskey AJ. Non-radioactive assay for Acetyl-CoA carboxylase activity. J. Oil Palm Res. Special Issue on Malaysia-MIT Biotechnology Partnership Programme V. 2008; 2: 30–36

32. Racagni GE, Machado de Domenech EE. Characterization of *Trypanosoma cruzi* hexokinase. Mol Biochem Parasitol. 1983; 9: 181–188. https://doi.org/10.1016/0166-6851(83)90108-1 PMID: 6366548

33. Rütti MF, Richard S, Penno A, von Eckardstein A, Hornemann T. An improved method to determine serine palmitoyltransferase activity. J Lip Res. 2009; 50: 1237–1244. https://doi.org/10.1194/jlr.D900001-JLR200 PMID: 19181628

34. Magdaleno A, Ahn IY, Paes LS, Silber AM. Actions of a proline analogue, L-thiazolidine-4-carboxylic acid (T4C), on *Trypanosoma cruzi*. PLoS One. 2009; 4: e4534–e4534. https://doi.org/10.1371/journal.pone.0004534 PMID: 19229347

35. Damasceno FS, Barison MJ, Pral EM, Paes LS, Silber AM. Memantine, an antagonist of the NMDA glutamate receptor, affects cell proliferation, differentiation and the intracellular cycle and induces apoptosis in *Trypanosoma cruzi*. PLoS Negl Trop Dis. 2014; 8: e2717–e2717. https://doi.org/10.1371/journal.pntd.0002717 PMID: 24587468

36. Figarella K, Rawer M, Uzcategui NL, Kubata BK, Lauber K, Madeo F, et al. Prostaglandin D2 induces programmed cell death in *Trypanosoma brucei* bloodstream form. Cell Death Differ. 2005; 12: 335–346. https://doi.org/10.1038/sj.cdd.4401564 PMID: 15678148

37. Lopaschuk GD, Wall SR, Olley PM, Davies NJ. Etomoxir, a carnitine palmitoyltransferase I inhibitor, protects hearts from fatty acid-induced ischemic injury independent of changes in long chain acylcarnitine. Circ Res. 1988; 63: 1036–1043. https://doi.org/10.1161/01.res.63.6.1036 PMID: 3197271

38. Koeller CM, Heise N. The sphingolipid biosynthetic pathway is a potential target for chemotherapy against Chagas disease. Enzyme Res. 2011; 2011: 1–13. https://doi.org/10.4061/2011/648159 PMID: 21603271

39. Divakaruni AS, Hsieh WY, Minarrieta L, Duong TN, Kim KKO, Desousa BR, et al. Etomoxir inhibits macrophage polarization by disrupting CoA homeostasis. Cell Metab. 2018; 28: 490–503.e497. https://doi.org/10.1016/j.cmet.2018.06.001 PMID: 30043752

40. Duszenko M, Figarella K, Macleod ET, Welburn SC. Death of a trypanosome: a selfish altruism. Trends Parasitol. 2006; 22: 536–542. https://doi.org/10.1016/j.pt.2006.08.010 PMID: 16942915

41. Mariano AC, Santos R, Gonzalez MS, Feder D, Machado EA, Piscarelli B, et al. Synthesis and mobilization of glycogen and trehalose in adult male *Rhodnius prolixus*. Arch Insect Biochem Physiol. 2009; 72: 1–15. https://doi.org/10.1002/arch.20319 PMID: 19514081

42. Ribeiro JMC, Genta FA, Sorgine MHF, Logullo R, Mesquita RD, Paiva-Silva GO, et al. An insight into the transcriptome of the digestive tract of the bloodsucking bug, *Rhodnius prolixus*. PLoS Negl Trop Dis. 2014; 8: e2594–e2594. https://doi.org/10.1371/journal.pntd.0002594 PMID: 24416461

43. Antunes L, Han J, Pan J, Moreira CJC, Azambuja P. Metabolic signatures of triatomine vectors of *Trypanosoma cruzi* unveiled by metabolomics. PLoS ONE. 2013; 8: 77283–77283. https://doi.org/10.1371/journal.pone.0077283 PMID: 24204787

44. Gondim KC, Atella GC, Pontes EG, Majerowicz D. Lipid metabolism in insect disease vectors. Insect Biochem Mol Biol. 2018; 101: 108–123. https://doi.org/10.1016/j.ibmb.2018.08.005 PMID: 30171905

45. Bittencourt-Cunha PR, Silva-Cardoso L, Oliveira GAd, Silva JRd, Silveira ABd, Kluck GEG, et al. Perimicrovillar membrane assembly: the fate of phospholipids synthesised by the midgut of *Rhodnius prolixus*. Mem Inst Oswaldo Cruz. 2013; 108: 494–500. https://doi.org/10.1590/S0074-02761080420130 16 PMID: 23827998

46. Wood DE. *Trypanosoma cruzi*: fatty acid metabolism *in vitro*. Exp Parasitol. 1975; 37: 60–66. https://doi.org/10.1016/0014-4894(75)90052-1 PMID: 1090440

47. Wood DE, Schiller EL. *Trypanosoma cruzi*: comparative fatty acid metabolism of the epimastigotes and trypomastigotes *in vitro*. Exp Parasitol. 1975; 38: 202–207. https://doi.org/10.1016/0014-4894(75)90022-3 PMID: 1100424

48. Cazzulo JJ. Aerobic fermentation of glucose by trypanosomatids. FASEB J. 1992; 6(13): 3153–3161. https://doi.org/10.1096/fasebj.6.13.1397837 PMID: 1397837

49. Frydman B, Santos C, Cannata JJB, Cazzulo JJ. Carbon-13 nuclear magnetic resonance analysis of [1-13C]glucose metabolism in *Trypanosoma cruzi*. Evidence of the presence of two alanine pools and of two CO2 fixation reactions. Europ J Biochem. 1990; 192: 363–368. https://doi.org/10.1111/j.1432-1033.1990.tb19235.x PMID: 2120054

50. Leroux AE, Maugeri DA, Opperdoes FR, Cazzulo JJ, Nowicki C. Comparative studies on the biochemical properties of the malic enzymes from *Trypanosoma cruzi* and *Trypanosoma brucei*. FEMS Microbiol Lett. 2011; 314: 25–33. https://doi.org/10.1111/j.1574-6968.2010.02142.x PMID: 21105905

51. Zelada C, Montemartini M, Cazzulo JJ, Nowicki C. Purification and partial structural and kinetic characterization of an alanine aminotransferase from epimastigotes of *Trypanosoma cruzi*. Mol Biochem Parasitol. 1996; 79: 225–228. https://doi.org/10.1016/0166-6851(96)02652-7 PMID: 8855559

52. Montemartini M, Buá J, Bontempi E, Zelada C, Ruiz AM, Santomé JA, et al. A recombinant tyrosine aminotransferase from *Trypanosoma cruzi* has both tyrosine aminotransferase and alanine aminotransferase activities. FEMS Microbiol Lett. 1995; 133: 17–20. https://doi.org/10.1111/j.1574-6968.1995.tb07854.x PMID: 8566704

53. Marciano D, Llorente C, Maugeri DA, de la Fuente C, Opperdoes F, Cazzulo JJ, et al. Biochemical characterization of stage-specific isoforms of aspartate aminotransferases from *Trypanosoma cruzi* and *Trypanosoma brucei*. Mol Biochem Parasitol. 2008; 161: 12–20. https://doi.org/10.1016/j.molbiopara.2008.05.005 PMID: 18602174

54. Cazzulo JJ, Arauzo S, Franke de Cazzulo BM, Cannata JJB. On the production of glycerol and L-alanine during the aerobic fermentation of glucose by trypanosomatids. FEMS Microbiol Lett. 1988; 51: 187–191.

55. Boveris A, Hertig CM, Turrens JF. Fumarate reductase and other mitochondrial activities in *Trypanosoma cruzi*. Mol Biochem Parasitol. 1986; 19: 163–169. https://doi.org/10.1016/0166-6851(86)90121-0 PMID: 3523239

56. Cazzulo JJ. Intermediate metabolism in *Trypanosoma cruzi*. J Bioenerg Biomembr. 1994; 26: 157–165. https://doi.org/10.1007/BF00763064 PMID: 8056782

57. Rogerson GW, Gutteridge WE. Catabolic metabolism in *Trypanosoma cruzi*. Int J Parasitol. 1980; 10: 131–135. https://doi.org/10.1016/0020-7519(80)90024-7 PMID: 6989775

58. Pereira MG, Visbal G, Salgado LT, Vidal JC, Godinho JLP, De Cicco NNT, et al. *Trypanosoma cruzi* epimastigotes are able to manage internal cholesterol levels under nutritional lipid stress conditions. PLoS ONE. 2015; 10: e0128949–e0128949. https://doi.org/10.1371/journal.pone.0128949 PMID: 26068009

59. Pereira MG, Visbal G, Costa TFR, Frases S, de Souza W, Atella G, et al. *Trypanosoma cruzi* epimastigotes store cholesteryl esters in lipid droplets after cholesterol endocytosis. Mol Biochem Parasitol. 2018; 224: 6–16. https://doi.org/10.1016/j.molbiopara.2018.07.004 PMID: 30016698

60. Allmann S, Mazet M, Ziebart N, Bouyssou G, Fouillen L, Dupuy JW, et al. Triacylglycerol storage in lipid droplets in procyclic *Trypanosoma brucei*. PLoS ONE. 2014; 9: e114628–e114628. https://doi.org/10.1371/journal.pone.0114628 PMID: 25493940

61. Alvarez VE, Kosec G, Sant'Anna C, Turk V, Cazzulo JJ, Turk B. Autophagy is involved in nutritional stress response and differentiation in *Trypanosoma cruzi*. J Biol Chem. 2008; 283: 3454–3464. https://doi.org/10.1074/jbc.M708474200 PMID: 18039653

62. Contreras VT, Salles JM, Thomas N, Morel CM, Goldenberg S. *In vitro* differentiation of *Trypanosoma cruzi* under chemically defined conditions. Mol Biochem Parasitol. 1985; 16: 315–327. https://doi.org/10.1016/0166-6851(85)90073-8 PMID: 3903496

63. Wainszelbaum MJ, Belaunzarán ML, Lammel EM, Florin-Christensen M, Florin-Christensen J, Isola ELD. Free fatty acids induce cell differentiation to infective forms in *Trypanosoma cruzi*. Biochem J. 2003; 375: 705–712. https://doi.org/10.1042/BJ20021907 PMID: 12887332

64. Contreras VT, Morel CM, Goldenberg S. Stage specific gene expression precedes morphological changes during *Trypanosoma cruzi* metacyclogenesis. Mol Biochem Parasitol. 1985; 14: 83–96. https://doi.org/10.1016/0166-6851(85)90108-2 PMID: 3885031

65. Homsy JJ, Granger B, Krassner SM. Some factors inducing formation of metacyclic stages of *Trypanosoma cruzi*. J Protozool. 1989; 36: 150–153. https://doi.org/10.1111/j.1550-7408.1989.tb01063.x PMID: 2657033

66. van Hellemond JJ, Opperdoes FR, Tielens AGM. The extraordinary mitochondrion and unusual citric acid cycle in *Trypanosoma brucei*. Biochem Soc Trans. 2005; 33: 967–967. https://doi.org/10.1042/BST20050967 PMID: 16246022

67. Docampo R, de Boiso JF, Stoppani AO. Tricarboxylic acid cycle operation at the kinetoplast-mitochondrion complex of *Trypanosoma cruzi*. Biochim Biophys Acta. 1978; 502: 466–476. https://doi.org/10.1016/0005-2728(78)90079-8 PMID: 350277

68. Bringaud F, Rivière L, Coustou V. Energy metabolism of trypanosomatids: Adaptation to available carbon sources. Mol Biochem Parasitol. 2006; 149: 1–9. https://doi.org/10.1016/j.molbiopara.2006.03.017 PMID: 16682088

69. Villafraz O, Biran M, Pineda E, Plazolles N, Cahoreau E, Souza ROO, et al. Procyclic trypanosomes recycle glucose catabolites and TCA cycle intermediates to stimulate growth in the presence of physiological amounts of proline. PLoS Pathog. 2021; 17: e1009204. https://doi.org/10.1371/journal.ppat.1009204 PMID: 33647053